

Authors response on Referee #1-2

Text in blue is original comment from referee followed by a reply and the actions done to improve the manuscript. A track-changes version of manuscript and supplemental are find at the end of the pdf.

Response to Anonymous Referee #1

General comments

This manuscript reports results of laboratory experiments on secondary organic aerosol (SOA) formation from the photooxidation of 1,3,5-trimethylbenzene (TMB). TMB is an SOA precursor emitted from anthropogenic sources. The authors employ an original flow reactor combined with a chemical ionization mass spectrometer to investigated effects of OH exposure and NO_x level on the distribution of oxidation products including particles, highly oxygenated molecules (HOMs), dimeric HOMs, and nitrated HOMs. They concluded that anthropogenic VOCs such as TMB could lead new particle formation (NPF) but NPF is suppressed under high NO conditions. The research subject of this study is paid central attention in the field of atmospheric chemistry. The authors employ cutting edge instruments and provide new physical insight into the field of atmospheric chemistry. Because flow reactor experiments under high NO_x conditions are very new, the authors should discuss difference between examined reaction conditions and ambient ones. This manuscript suits for the scope of this journal and will be publishable after revisions are made by taking into account reviewer's comments.

Major comments:

(1) Please describe ozone concentration data in the text to discuss the reaction of remaining ozone with NO. If ozone level is higher than 50 ppb, the reaction of ozone with NO (with the rate constant of $1.8 \times 10^{-14} \text{ cm}^3 \text{ molecule}^{-1} \text{ s}^{-1}$) can significantly occur within a reaction time of 34 s, and NO is converted to NO₂. The authors primary assume that nitrated HOMs are formed from the reactions of HOM-RO₂ radicals with NO. However, formation of peroxy nitrates from the reactions of HOM-RO₂ with NO₂ or formation of nitrates from the reactions of HOM-RO with NO₂ might be important if NO₂ level is much higher than NO level. In experiments with NO_x under high ozone levels, NPF was observed. These results may suggest that NO become very low levels due to the reaction with ozone within the reaction time of 34 s, and the reactions of HOM-RO₂ with NO₂ may become more important than the reactions of HOM-RO with NO.

Reply: Yes, the titration of NO with ozone is a concern. However, as shown in a new Figure (S3) there is still some NO left at the end of the flow reactor. i.e. after 34 s there is still NO available to react with any HOM-RO₂.

In the experiment with NO_x in which NPF was observed, the NO_x concentration was the lowest and the OH exposure was the highest among the experiments with NO_x (Table 1). In addition, the ten compounds with the highest contribution includes only one nitrogen-containing compound, in contrast to the other NO_x experiments where the nitrogen-containing compounds were the majority of the top ten (Table S1). This makes us to conclude that the OH concentration was high enough to lead to the formation of more oxidized products, by allowing a second OH reaction to take place, and the formation of dimers which are more

likely to contribute to NPF rather than products from the reaction of HOM-RO₂ with NO or NO₂.

Action: A new Figure (S3) is added to the SI. New text is added to elucidate the effect of titration and the remaining NO.

“As already has been described NO_x was introduced to the Go:PAM as NO. After the addition of ozone, the ozone concentration decreases from 100 ppb to ~80 ppb at the experiment with lower NO_x levels and to ~50 ppb at the experiment with higher NO_x levels, as it reacts with NO producing NO₂. For both high and low NO_x conditions there is NO left after the initial reaction with ozone (see grey areas of Figure S3).”

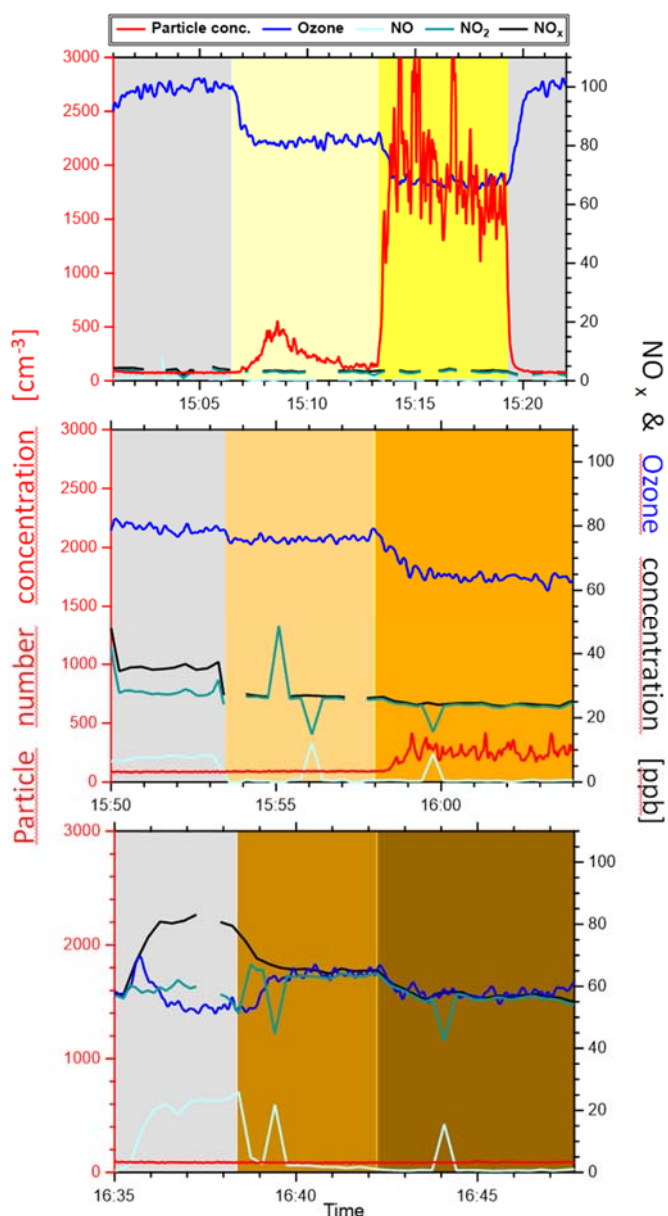


Figure S3: Particle number (red), ozone (blue), NO_x (black), NO (light blue) and NO₂ (cyan) concentrations under NO_x free conditions (top panel), initial NO_x:VOC≈1 (middle panel) and NO_x:VOC≈3 (bottom panel). The grey areas represent dark conditions, the light yellow, orange and brown represent lower OH exposure conditions (using one UV lamp) and the dark yellow, orange and brown represent higher OH exposure conditions (using two UV lamps).

(2) The authors use NO_x levels of 35-82 ppbv, which are similar to NO_x levels in urban air, whereas they use HO_x (including OH and HO₂) levels much higher than ambient levels to accelerate reactions in the laboratory. These conditions may result in overestimation of HOM-RO₂ + HO₂ reactions and underestimation of HOM-RO₂ + NO, HOM-RO₂ + NO₂, and HOM-RO₂ autoxidation, compared to ambient conditions. The authors should discuss difference in branching of HOM-RO₂ reactions between present laboratory conditions and ambient conditions.

Reply: Yes, there could be an overrepresentation of HO_x chemistry relative to NO_x. However, the idea is to indicate a shift from HO_x to NO_x chemistry so the effect observed might be even more pronounced in polluted environments.

Action: New text is added in the atmospheric implication and conclusion section:

“The experimental designed using the Go:PAM with concentrations of HO_x (and RO_x) higher than ambient would attenuate the influence of added NO_x. This will further emphasis the implication of our findings and most likely the NO_x effect would be even more important in the urban atmosphere.”

(3) The authors assume that nitrogen-containing products formed from the oxidation of TMB in the presence of NO_x are nitrates or peroxy nitrates; however this is not evident and further discussion will be necessary in the text. Basically the reviewer agrees with authors' assumption, but in general major nitrogen-containing products, formed from the oxidation of aromatic hydrocarbons, are nitro-aromatic compounds. 1,3,5-Trimethylbenzene is highly methyl-substituted aromatic hydrocarbon and multiple methyl groups inhibit formation of nitro-aromatic compounds (Sato et al., 2012). At this point of view, TMB employed in this study is not a typical aromatic hydrocarbon and a specific molecule, which barely lead to formation of nitro-aromatic compounds.

Reply: We agree with the reviewer that nitro-aromatic compounds are quite unlikely to be formed from TMB (Sato et al., 2012). Aromaticity will get lost before initial products react with NO. That's why we assume that's addition of NO_x leads to organonitrates (RONO₂) or peroxy nitrates (ROONO₂), with higher contribution from the RONO₂. We also agree that a schematic with proposed reaction mechanisms for the formation of organonitrates will be beneficial to illustrate this.

Action: A figure with a proposed formation mechanism of organonitrates is now included (Figure 5).

The following sentences are included:

“These compounds are expected to be nitrates or peroxy nitrates, as it is highly unlikely to form nitro-aromatic compounds from TMB (Sato et al., 2012).”

“A proposed detailed reaction mechanism is depicted in Figure 5.”

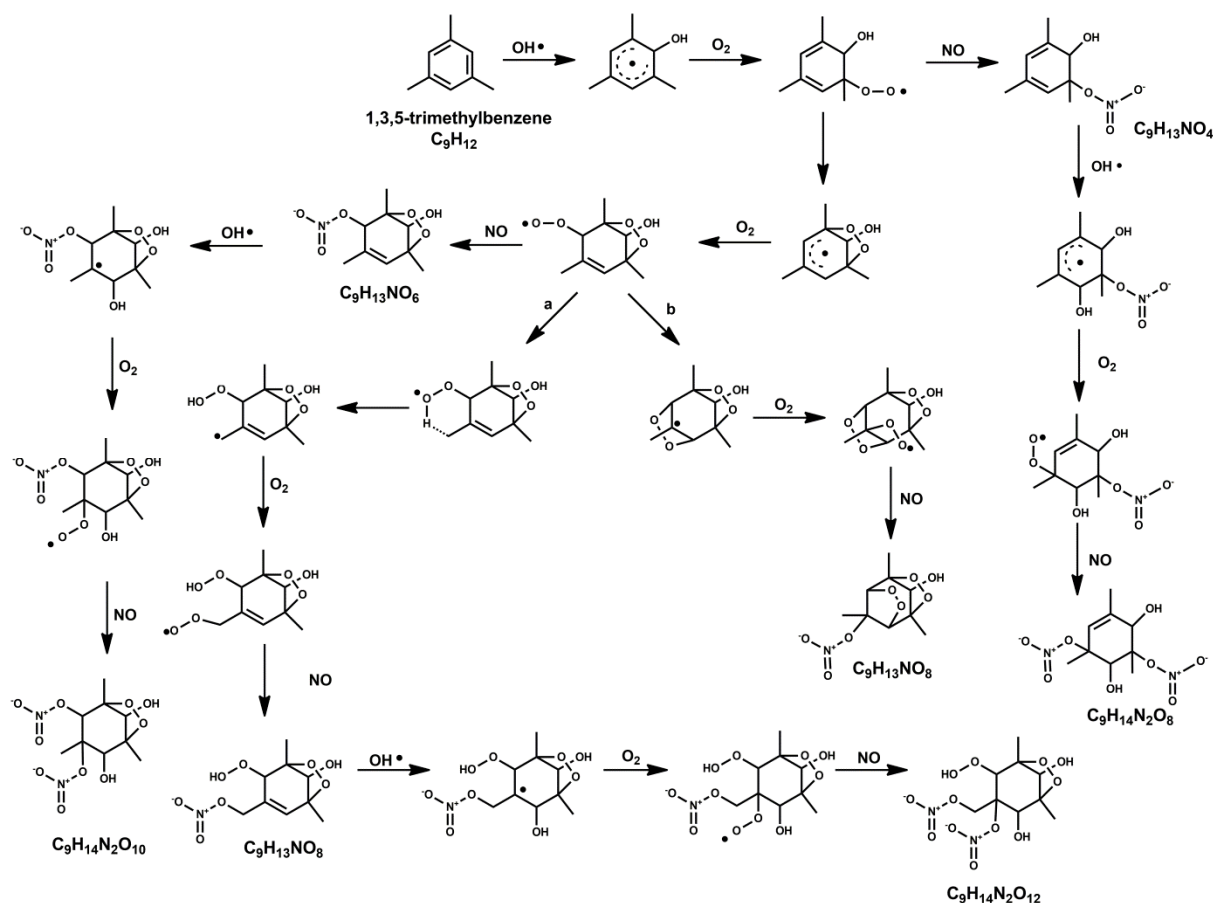


Figure 5: The proposed radical reaction mechanism for the formation of some of the mono- and di-nitrates from TMB mentioned in this study. Two separate mechanisms were suggested for the species with the formula $C_9H_{13}NO_8$, which formation pathways are based on (a) (Wang et al., 2017) and (b) (Molteni et al., 2018).

Specific comments:

(4) Page 3, line 14 and reference list in page 18. Sato et al., 2018 should be Sato et al., 2012

Action: Done.

(5) Page 3, line 32. In the unit, “L mol⁻¹”, “-1” should be superscript.

Action: Done.

(6) Page 4, lines 1-5. Please discuss the phase of products detected by API-TOFMS. If it detects products in the aerosol phase, how were these particulate products vaporized in the ion source? Brief explanations would be necessary in the text.

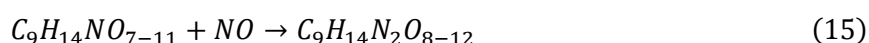
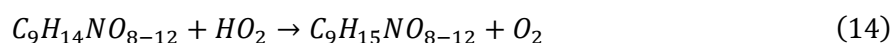
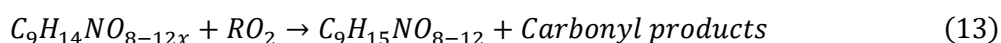
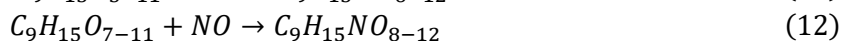
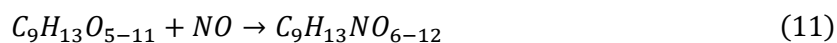
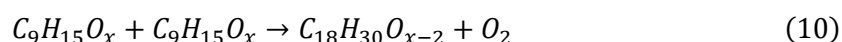
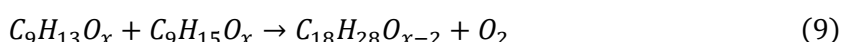
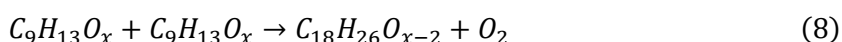
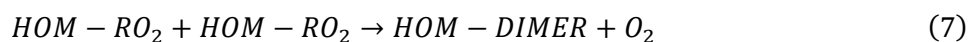
Reply: Only the gas phase oxidation products are detected by the API-TOFMS.

Action: It is now clarified in the text that the detected products are measured in the gas-phase. “Gas phase oxidation products were measured...”

(7) Page 9, lines 14-15. The formation process of compounds with 12 H and 16 H should be explained more in detail. For example, the words, “(terminated from $C_9H_{13}O_x$ radicals)”, should be written as “(formed from the $C_9H_{13}O_x + RO_2 \rightarrow C_9H_{12}O_{x-1} + ROH + O_2$ reaction)”.

Reply: ok

Action: Selected reactions have been added to the text. See Reactions 3-15.



(8) Page 9, lines 32-34. C₉H₁₄O_x products include first-generation and second generation products, i.e., these are formed from the C₉H₁₃O_{x+1} + RO₂ -> C₉H₁₄O_x + R'CHO + O₂ reaction as well as C₉H₁₅O_{x+1} + RO₂ -> C₉H₁₄O_x + ROH + O₂ reaction. Please explain why C₉H₁₄O_x products have mainly characteristics of second generation products.

Reply: That's true C₉H₁₄O_x products can be either first or second generation products. They have mainly characteristics of secondary products, as their contribution to the top ten compounds (Table S1) increases for the experiments with higher OH exposures, in which more oxidized products can be formed.

Action: The text now includes the following:

"C₉H₁₄O_x can be either first or second generation products and originate from either C₉H₁₃O_x or C₉H₁₅O_x (reactions 5 and 6)."

"The C₉H₁₄O_x products have mainly characteristics of second generation products, as their contribution is enhanced in the experiments with higher OH exposures (Table S1), in which there is an enhanced possibility for secondary chemistry initiated by reaction of OH with the first generation products."

(9) Page 9, last sentence. The authors describe "the contribution of C₉H₁₅O_x is reduced at expense of C₉H₁₄O_x and C₉H₁₆O_x – HOM and dimers," but the meaning of this sentence is unclear. Do the authors mean that the contribution of C₉H₁₅O_x is reduced at the expense of C₉H₁₄O_x and C₉H₁₆O_x?

Reply: Maybe unclear but we were arguing that the formation of secondary products (C₉H₁₄O_x & C₉H₁₆O_x), due to higher OH exposure, is responsible for the reduction of the C₉H₁₅O_x radicals.

Action: We modify the text as following: “At the highest OH exposures in exp 4, the contribution of C₉H₁₅O_x radicals, one of the top ten contributors to the signal (Table S1), is reduced, while the contribution of the second generation products (C₉H₁₄O_x and C₉H₁₆O_x) and dimers increases.”

(10) Page 12, line 20. The reviewer cannot find “Figure 7.”

Reply: Figure 7 was missed out but should have been found in the supplemental as Figure S3.

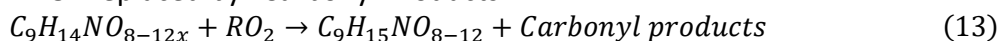
Action: The missed out Figure 7 is now included in the Supplementary Information as Figure S3.

(11) Page 13, line 4. The description, “hydroxyl”, should be “RO₂”.

Action: ...Via “peroxy”... is included in the text.

(12) Page 13, eq. (6). The chemical formula, R=O, would not be accurate. If the authors use “R=O”, please explain that R=O represents carbonyl products.

Action: “R=O” replaced by “Carbonyl Products”.



(13) Page 13, line 29. Please correct “reaction 56”.

Reply: The “reaction 56” refers to the corresponding reaction in Table S2. The rate coefficient that is used is based on the recommended one from Berndt et. (2018)

Action: The text has been corrected accordingly.

“b) the rate coefficient ($1.0 \times 10^{-11} \text{ cm}^3 \text{ molecules}^{-1} \text{ s}^{-1}$) from Berndt et al. (2018) for HOMRO₂ + NO with a branching ratio of 0.3 for ON formation (reaction 56 in Table S2).”

(14) Page 15, line 15. “Wang et al. (2018)” should be “Wang et al. (2017)”.

Action: Done.

(15) The caption of FigureS1. In the caption it is explained “Bottom: Modelled product distribution for all 8 experiments”, but the reviewer cannot find this bottom figure.

Reply: The caption “Bottom: Modelled...experiments with NO_x.” is referring to the Figure 5 in the main text.

Action: It is now corrected.

“Figure S1: Vertical profile of TMB (ppb) in the PAM chamber without (left) and with NO_x (right).”

(16) Table S2. The symbol, “=”, represents reversible reaction if it is used in reaction equations. The reviewer recommends for the authors to use arrow symbols instead.

Reply: We agree.

Action: Done.

Response to Anonymous Referee #2

General comments

This manuscript investigates the formation of highly oxygenated molecules (HOMs) from the oxidation of TMB under different conditions (i.e., OH exposure and NO_x concentrations). The

HOMs are measured by a NO₃- CIMS and the distributions of HOMs species under different reaction conditions are reported. As there are few studies on the HOMs from aromatics oxidation, these results are worthy to be documented. The major finding is that NO_x inhibits the formation of HOMs and enhances the formation of organonitrates, by altering the RO₂ chemistry. The experiments are nicely designed and conducted and the manuscript is clearly written. I recommend publication after major revision.

Major comments:

1. In the kinetic model, the oxidized peroxy radicals (HOMRO₂) were considered to be formed after 3 autoxidation steps of a general RO₂ with a rate constant of 0.1667 s⁻¹. This rate is inferred from α-pinene + O₃ RO₂. However, the isomerization rate of biogenic RO₂ is generally not applicable to aromatic RO₂, because of the presence of C-C double bonds in aromatics. The isomerization rate of the TMB-OH-OO to bicyclic alkyl radical could be on the order of 1000 s⁻¹ 1-2. For the second isomerization step (i.e., potentially form a tricyclic alkyl radical), the rate is uncertain, but is likely much larger than 0.17 s⁻¹ 3. Even though there are large uncertainties in the RO₂ isomerization rates, more appropriate values should be used. A book chapter by Vereecken et al.³ has a nice summary on this topic.

In fact, the tuning of the photon flux to match the measured decay of O₃ may be related to the poor representation of RO₂ chemistry.

Reply: Yes, this part could be more elaborated. A comment is that even if the first step is very fast the following two steps will be rate limiting steps reducing the rate of the overall three step process and might be approaching our rather slow reaction rate used. However, we have now considered this more thoughtfully and the resulting rate of the reaction used in the simplified model has been increased with a factor of 2 (however, the product distributions are more or less in line with original model and support our general conclusions).

The considerations were:

According to the oxygen content in the majority of the C₉ products the oxidized peroxy radicals (HOMRO₂) should contain either seven, nine or eleven oxygens which would be formed after two, three and four autoxidation steps, respectively. To simplify the model the produced HOMRO₂ in the model were assumed to be formed after 3 autoxidation steps. As pointed out by the referee it is not as simple as each step has the same rate coefficient. However, there are large uncertainties where our best estimate would be the following assumptions. The 1st step where the O₂ group make a bicyclic radical has a large rate coefficient where Jenkin et al., 2019 suggests a rate coefficient for similar reaction to be larger than 3.6 x 10² s⁻¹ (Jenkin et al., 2019). For the 2nd step we assume an internal hydrogen shift potentially facilitated by a conjugated three carbon system. Here Wang et al., 2017 give a large range in reaction rates for similar reactions where the radical from toluene is slow (2.6 x 10⁻²) while the radical from larger compounds has higher values (e.g. 7.0 s⁻¹). We use a value of 1 s⁻¹ to represent this step. For the final 3rd step that would represent another hydrogen shift we use the value of 0.5 s⁻¹ originally suggested in the paper by Ehn et al., 2014. The combined rate of these three subsequent steps would then be 0.33 s⁻¹. This value is a factor of 2 higher than the original value but does not dramatically change our conclusions from the model experiments.

Action: The rate of this reaction has been increased in the model and new text has been added to describe the motivation of using such rate for this parametrized three step reaction.

“According to the oxygen content in the majority of the C₉ products the oxidized peroxy radicals (HOMRO₂) should contain either seven, nine or eleven oxygen which would be formed

after two, three or four autoxidation steps, respectively. To simplify the model the produced HOMRO₂ in the model were assumed to be formed after 3 autoxidation steps. There are large uncertainties on estimating the rate coefficients for the autoxidation step (Jenkin et al., 2019). The following assumptions were taken in account for our best lumped estimation of the three step oxidation. The 1st step where the O₂ group make a bicyclic radical most likely has a large rate coefficient where Jenkin et al., 2019 suggests a rate coefficient for similar reactions to be larger than $3.6 \times 10^2 \text{ s}^{-1}$ (Jenkin et al., 2019). For the 2nd step we assume an internal hydrogen shift potentially facilitated by a conjugated three carbon system. Here Wang et al., 2017 give a large range in reaction rates for similar reactions where the radical from toluene is slow ($2.6 \times 10^{-2} \text{ s}^{-1}$) while the radical from larger compounds has higher values (e.g. 7.0 s^{-1}). We use a value of 1 s^{-1} to represent this 2nd step. For the 3rd step that would represent another hydrogen shift we use the value of 0.5 s^{-1} originally suggested in the paper by Ehn et al., 2014. The combined rate of these three subsequent steps would then be 0.33 s^{-1} ."

The relative contribution of the HOM monomers and dimers as well as the nitrated compounds using the new rate coefficient is shown in incorporated in the new Figure 2 (Panel B).

"Calculated concentrations for dimers are similar in exp 3 and higher in exp 4, compared to monomers."

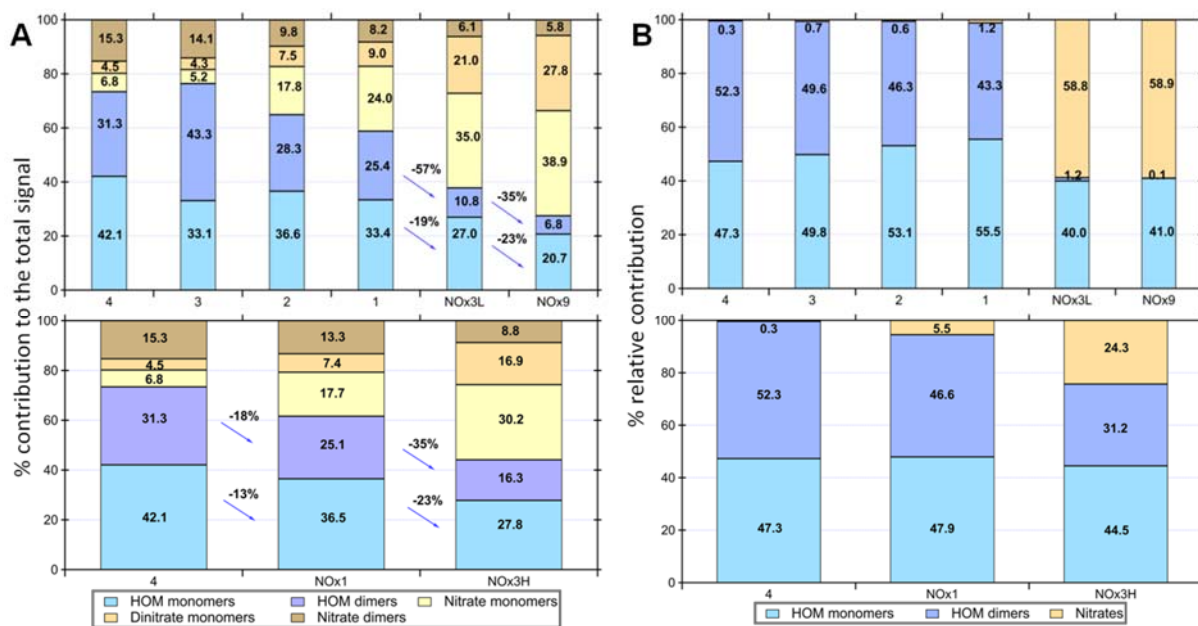


Figure 1: A) Overview of different compound groups to the total explained signal. Top panel illustrates the influence of a decrease of OH exposure (exp 4 - exp 1) and further decrease after adding NO_x in exp NO_x3L – exp NO_x9. Dimers show a larger relative reduction than monomers with increasing NO_x/VOC. Bottom panel shows the influence of increased NO_x/VOC on the product distribution. Experiments 4, 3 and NO_x1 resulted in particle formation. B) Modelled product distribution shown as lumped categories of nitrated compounds, HOM monomers and dimers and their relative contributions.

2. The authors compare observed HOMs distribution with that in Molteni et al. (2018) and noticed many important discrepancies. The authors must discuss potential causes for the discrepancies.

Reply: The experimental conditions and set up are the most important reasons. The Molteni et al. study react only a fraction of the TMB and would thus not form so many secondary products as in the current study. Their initial TMB concentration is 3 times higher (100ppb) compared to our study (30ppb) while the residence time is almost half, 20 sec compared to 34 sec. This may explain the formation of more oxidized compounds, especially more oxidized dimers. In addition, in Molteni et al. the OH radicals are produced outside of the flow tube (see Figure 1 at Molteni et al., 2018), then pre-mixed with the sample flow before the flow reactor. This, in conjunction with the higher TMB initial concentration, may lead to an early consumption of the OH radicals in the initial part of the flow reactor (see Figure S1-1, Supplement at Molteni et al., 2018) minimizing further oxidation, while in our study the OH radicals are produced inside the flow reactor, allowing a higher and more evenly distribution of OH radical concentrations in the flow reactor also favoring secondary reactions.

The formation of new particles in the flow reactor can change the HOM distribution, especially the dimers (Mohr et al., 2017), due to condensational sink. In our study one can see this effect in Figure 3. The product distribution depends on the OH concentration levels as well as on the particle number concentration. A direct comparison to Molteni et al. is not possible, as no values for the particle number concentration are reported. But for the given values of initial TMB (100ppb) and OH (higher than our highest value) concentrations a high particle concentration is expected. This large particle concentration may increase the dimer loss, change the product distribution pattern and make the comparison to our study more difficult. The relative humidity is another parameter which was different during the two studies (75% in Molteni et al., 38% in this study).

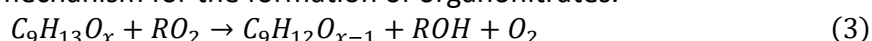
Despite these differences the conclusion is the same in both studies, that TMB under NO_x free conditions can rapidly form HOM of very low volatility, as they can initiate NPF.

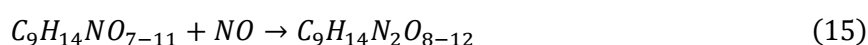
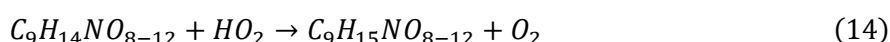
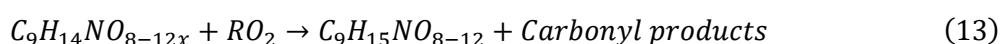
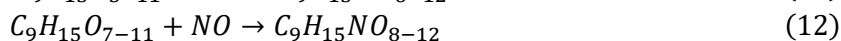
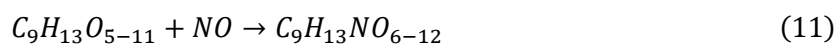
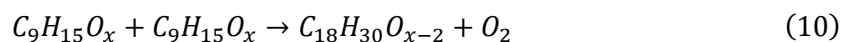
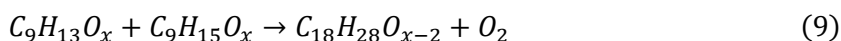
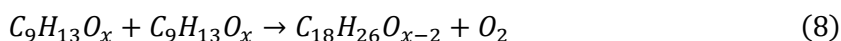
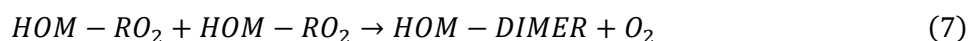
Action: The following text has been added to explain the potential discrepancies.

“These differences can be the result of different experimental conditions and set up. In our study the residence time is almost the double compared to Molteni et al., leading to the formation of more oxidized compounds, especially more oxidized dimers, which have been reported in this study. In addition, we produce OH radicals in the full length of the flow reactor enhancing the effects of secondary chemistry. Despite these differences there is a general agreement on the conclusions for NO_x free conditions with the Molteni study where one rapidly form HOM of very low volatility, that can initiate NPF.”

3. Reaction schematics on the formation mechanism of key HOMs monomer and dimers should be added. This is clearer than describing the mechanism with words.

Action: Reaction equation have been included (Reactions 3-15), as well as a figure (Figure 5) with a proposed reaction mechanism for the formation of organonitrates.





“A proposed detailed reaction mechanism is depicted in Figure 5.”

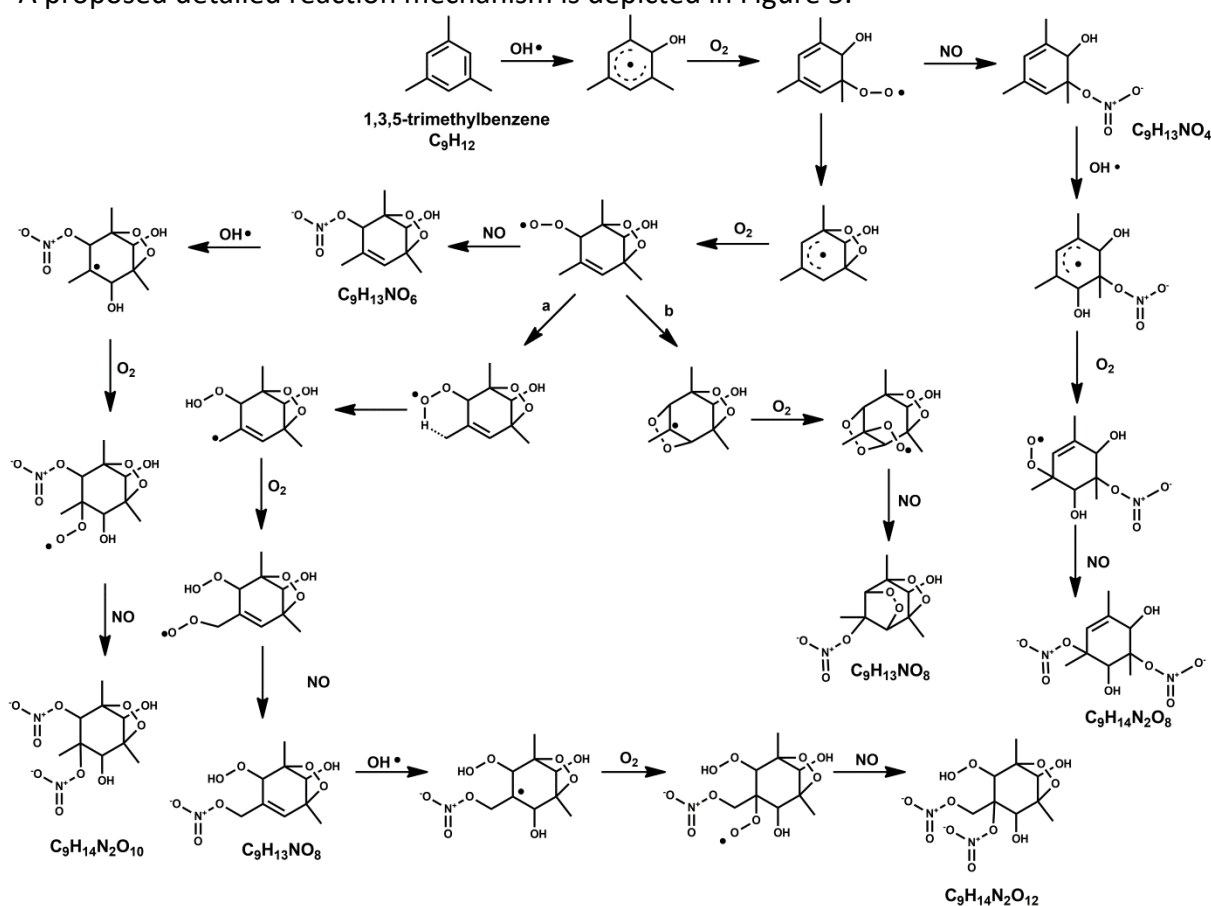


Figure 5: The proposed radical reaction mechanism for the formation of some of the mono- and di-nitrates from TMB mentioned in this study. Two separate mechanisms were suggested for the species with the formula C₉H₁₃NO₈, which formation pathways are based on (a) (Wang et al., 2017) and (b) (Molteni et al., 2018).

Minor comments

1. How is NO_x added into the reactor? I can't find the information in the method section nor schematic figure.

Action: "...while NO was introduced via a NO gas cylinder." is added to the main text.

2. Page 12 Line 18-20. Figure 7 is not in the manuscript. Also, it is highly unlikely that the ON yield from RO₂+NO is closed to unity

Reply: Figure 7 was missed out but should have been found in the supplemental as Figure S3.

Action: A new Figure S3 is now included in the Supplementary Information. New text reads: "The yield of ON from NO+RO₂ might be high based on the measurable increase of ON and the decrease of NO_x in the system (see **Error! Reference source not found.**)"

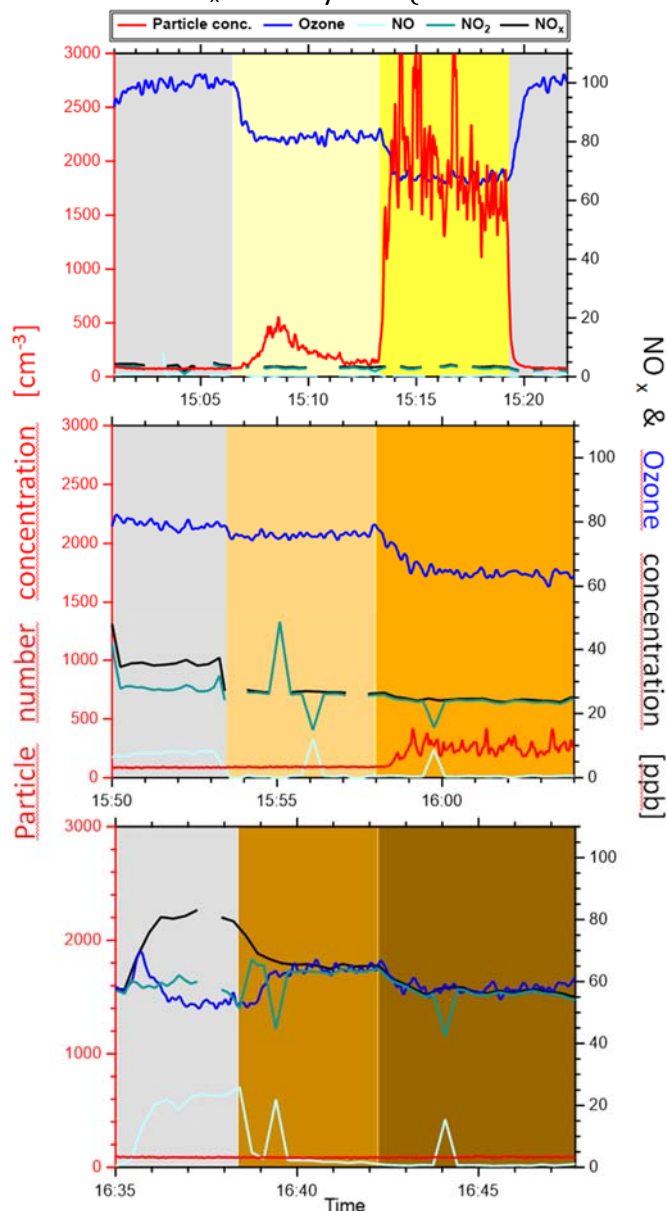


Figure S3: Particle number (red), ozone (blue), NO_x (black), NO (light blue) and NO₂ (cyan) concentrations under NO_x free conditions (top panel), initial NO_x:VOC \approx 1 (middle panel) and NO_x:VOC \approx 3 (bottom panel). The grey areas represent dark conditions, the light yellow, orange and brown represent lower OH exposure conditions (using one UV lamp) and the

dark yellow, orange and brown represent higher OH exposure conditions (using two UV lamps).

3. Page 12 Line 32. $C_9H_{13}O_5$ is formed after one isomerization step (i.e., initial OH addition, O_2 addition, RO_2 isomerization, and O_2 addition), not two steps.

Reply: That's true.

Action: New text reads: "one autoxidation step"

4. Page 13 Line 1. What do authors mean by "the formation of RO_2 precursor species with lower O numbers"? $C_9H_{15}O_{7-8}$ has many O atoms.

Reply: Yes, this is a relative term referring to comparison with other systems, yielding higher number of oxygen but was not clear from the content.

Action: We have now modified the text.

"The formation of RO_2 precursor species with 7-8 O numbers, i.e. $C_9H_{15}O_{7-8}$ likely stem from compounds terminated earlier in the radical chain process ($C_9H_{14}O_{4-5}$), which do not fall in the typical HOM class ($O:C \geq 6:9$)."

5. Page 13 Line 26. Zhang et al. (2018) is not in the reference list.

Action: Done. It is actually Zhao et al. (2018).

6. Figure 5 should be combined with figure 2 somehow to facilitate the comparison.

Reply: Ok.

Action: Figure 5 is now merged with Figure 2.

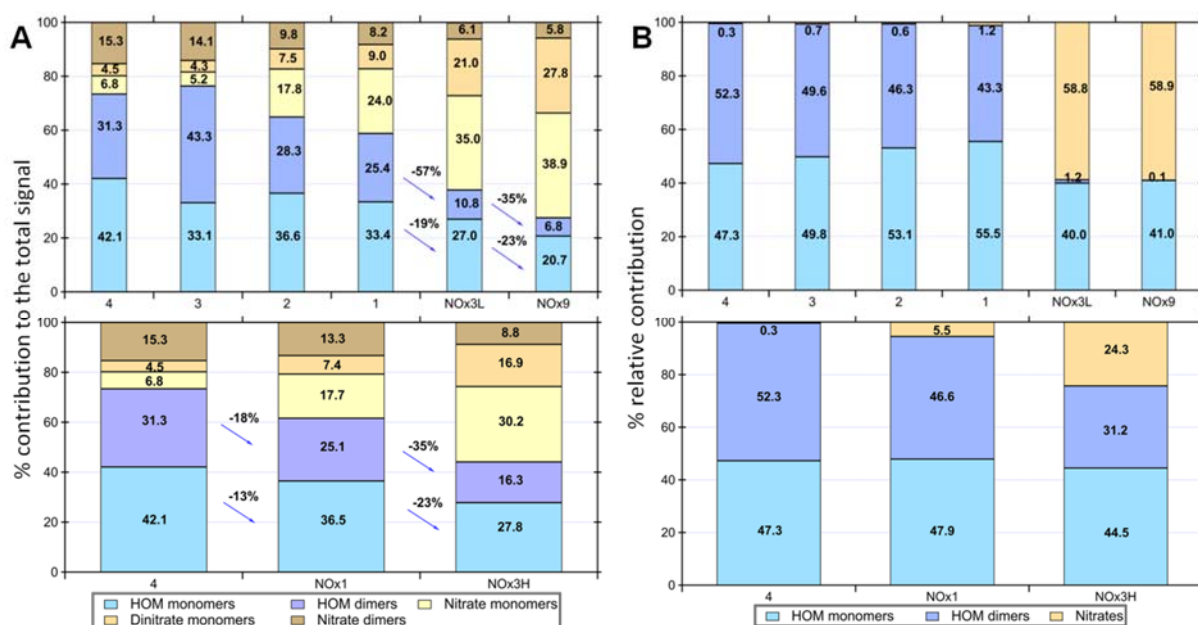


Figure 2: A) Overview of different compound groups to the total explained signal. Top panel illustrates the influence of a decrease of OH exposure (exp 4 - exp 1) and further decrease after adding NO_x in exp NO_x3L – exp NO_x9 . Dimers show a larger relative reduction than monomers with increasing NO_x/VOC . Bottom panel shows the influence of increased NO_x/VOC on the product distribution. Experiments 4, 3 and NO_x1 resulted in particle formation. B) Modelled product distribution shown as lumped categories of nitrated compounds, HOM monomers and dimers and their relative contributions.

References:

1. Ehn, M., Thornton, J. A., Kleist, E., Sipila, M., Junninen, H., Pullinen, I., Springer, M., Rubach, F., Tillmann, R., Lee, B., Lopez-Hilfiker, F., Andres, S., Acir, I. H., Rissanen, M., Jokinen, T., Schobesberger, S., Kangasluoma, J., Kontkanen, J., Nieminen, T., Kurten, T., Nielsen, L. B., Jorgensen, S., Kjaergaard, H. G., Canagaratna, M., Maso, M. D., Berndt, T., Petaja, T., Wahner, A., Kerminen, V. M., Kulmala, M., Worsnop, D. R., Wildt, J., and Mentel, T. F.: A large source of low-volatility secondary organic aerosol, *Nature*, 506, 476-479, 10.1038/nature13032, 2014.
2. Jenkin, M. E.; Valorso, R.; Aumont, B.; Rickard, A. R., Estimation of rate coefficients and branching ratios for reactions of organic peroxy radicals for use in automated mechanism construction. *Atmos. Chem. Phys.* 2019, 19, 7691-7717.
3. Mohr, C., Lopez-Hilfiker, F. D., Yli-Juuti, T., Heitto, A., Lutz, A., Hallquist, M., D'Ambro, E. L., Rissanen, M. P., Hao, L. Q., Schobesberger, S., Kulmala, M., Mauldin, R. L., Makkonen, U., Sipila, M., Petaja, T., and Thornton, J. A.: Ambient observations of dimers from terpene oxidation in the gas phase: Implications for new particle formation and growth, *Geophys Res Lett*, 44, 2958-2966, 10.1002/2017gl072718, 2017.
4. Molteni, U., Bianchi, F., Klein, F., El Haddad, I., Frege, C., Rossi, M. J., Dommen, J., and Baltensperger, U.: Formation of highly oxygenated organic molecules from aromatic compounds, *Atmospheric Chemistry and Physics*, 18, 1909-1921, 10.5194/acp-18-1909-2018, 2018.
5. Sato, K., Takami, A., Kato, Y., Seta, T., Fujitani, Y., Hikida, T., Shimono, A., and Imamura, T.: AMS and LC/MS analyses of SOA from the photooxidation of benzene and 1,3,5-trimethylbenzene in the presence of NO_x: effects of chemical structure on SOA aging, *Atmos. Chem. Phys.*, 12, 4667-4682, 10.5194/acp-12-4667-2012, 2012.
6. Wang, S., Wu, R., Berndt, T., Ehn, M., and Wang, L.: Formation of Highly Oxidized Radicals and Multifunctional Products from the Atmospheric Oxidation of Alkylbenzenes, *Environ Sci Technol*, 51, 8442-8449, 10.1021/acs.est.7b02374, 2017.

Effect of NO_x on 1,3,5-trimethylbenzene (TMB) oxidation product distribution and particle formation

[Epameinondas Tsiligiannis¹](#), Julia Hammes¹, ~~[Epameinondas Tsiligiannis¹](#)~~, [Christian Mark Salvador¹](#), Thomas F. Mentel^{1,2}, Mattias Hallquist^{1*}

¹Department of Chemistry and Molecular Biology, University of Gothenburg, Gothenburg, Sweden

²Institute of Energy and Climate Research, IEK-8: Troposphere, Forschungszentrum Jülich GmbH, Jülich, Germany

* Correspondence to: hallq@chem.gu.se

Abstract

Secondary organic aerosol (SOA) represents a significant fraction of the tropospheric aerosol and its precursors are volatile organic compounds (VOC). Anthropogenic VOCs (AVOC) dominate the VOC budget in many urban areas with 1,3,5-trimethylbenzene (TMB) being among the most reactive aromatic AVOCs. TMB formed highly oxygenated organic molecules (HOM) in NO_x free environment, which could contribute to new particle formation (NPF) depending on oxidation conditions were elevated OH oxidation enhanced particle formation. The experiments were performed in an oxidation flow reactor, the Go:PAM unit, under controlled OH oxidation conditions. By addition of NO_x to the system we investigated the effect of NO_x on particle formation and on the product distribution. We show that the formation of HOM and especially HOM accretion products, strongly varies with NO_x conditions. We observe a suppression of HOM and particle formation with increasing NO_x/ΔTMB and an increase in the formation of organonitrates (ON) mostly at the expense of HOM accretion products. We propose reaction mechanisms/pathways that explain the formation and observed product distributions with respect to oxidation conditions. We hypothesize that, based on our findings from TMB oxidation studies, aromatic AVOCs may not contribute significantly to NPF under typical NO_x /AVOC conditions found in urban atmospheres.

1 Introduction

Volatile organic compounds (VOC) are ubiquitous in the atmosphere and major precursors for secondary organic aerosol (SOA). SOA represents a dominant fraction of the tropospheric aerosol (Hallquist et al., 2009; Shrivastava et al., 2017; Gentner et al., 2017) and affects climate (Intergovernmental Panel on Climate, 2014) and health (WHO, 2016). Consequently research interest in SOA formation and properties is ranging from remote atmospheres (Ehn et al., 2012; Ehn et al., 2014; Kristensen et al., 2016) to densely populated and polluted environments (Chan and Yao, 2008; Hu et al., 2015; Guo et al., 2014; Hallquist et al., 2016). Following the study by Ehn et al. (Ehn et al., 2012), highly oxygenated organic molecules (HOM) with low volatilities, formed from the oxidation of biogenic volatile organic compounds (BVOCs), have attracted much research interest (Crouse et al., 2013; Ehn et al., 2014; Jokinen et al., 2014; Jokinen et al., 2015; Mentel et al., 2015; Yan et al., 2016; Berndt et al., 2016; Bianchi et al., 2019). These compounds have been shown to contribute to new particle formation (NPF) and to SOA growth (Ehn et al., 2014; Bianchi et al., 2016; Kirkby et al., 2016; Trostl et al., 2016; McFiggans et al., 2019), making them an important factor in the formation of atmospheric SOA. These oxidation products can be either described as HOM based on their high oxygen number ($O > 6$) (Bianchi et al., 2019) or as extremely low volatile organic compounds (ELVOC) based on their volatility (Donahue et al., 2012; Trostl et al., 2016). In this study, we will refer to oxidation products as HOM, because not all of the measured compounds may fulfill the criteria for ELVOC (Trostl

et al., 2016; Kurtén et al., 2016). Gas phase autoxidation of alkylperoxy radicals (RO_2) has been proposed as the formation mechanism for HOM (Crouse et al., 2013; Ehn et al., 2014; Jokinen et al., 2014). After the initial reaction of an oxidant with the VOC and subsequent addition of O_2 to the alkylradical (R), the produced RO_2 isomerizes via intra molecular H abstraction (H-shift). During this process a hydroperoxide group and a new R is formed. Additional O_2 addition and H-shift sequences can introduce large amounts of oxygen to the molecule and subsequently lower the vapour pressure. The chemistry of aromatic compounds is somewhat different compared to other VOCs as they can lose their aromaticity during the initial OH attack while they can retain the ring structure. Moreover, reaction products are more reactive than the parent compound. The produced RO_2 form an oxygen bridge, a bicyclic and potentially a tricyclic alkylradical (Molteni et al., 2018; Wang et al., 2017) before further oxidation processes open the ring structure. For 1,3,5-trimethylbenzene (TMB), emitted from combustion sources in the urban environment, Molteni et al. (2018) proposed a generalized reaction scheme for HOM formation after OH addition. According to their scheme, first generation alkylperoxy radicals with the general formula of $C_9H_{13}O_{5-11}$ were formed from the initial OH attack and subsequent H shift and O_2 addition sequences. A postulated second OH attack would result in propagating peroxy radical chains yielding radicals with the general formulas $C_9H_{15}O_{7-11}$.

Generally, the termination reaction of RO_2 (with a general $m/z = x$) with HO_2 , leads to the formation of hydro peroxides ($m/z = x + 1$) while termination reactions with other RO_2 can lead to the formation of a carbonyl ($m/z = x - 17$), a hydroxy group ($m/z = x - 15$) or dimers ($m/z = 2x - 32$) (Mentel et al., 2015; Jokinen et al., 2014; Rissanen et al., 2014). The propagation reaction of RO_2 with another RO_2 or NO also results in the formation of RO ($m/z = x - 16$). The RO can undergo internal H shift leading to the formation of a hydroxy group and subsequent a new peroxy radical which can continue the autoxidation sequences. The alkoxy step shifts of the observed m/z by 16 leads to overlap of different termination product sequences. During extensive oxidation the first generation products are subject to secondary chemistry increasing the numbers of products. Molteni et al. (Molteni et al., 2018) found several closed shell monomer products with the general formula $C_9H_{12-16}O_{5-11}$ from the oxidation of TMB with OH. The formation of dimers with different number of H atoms in their study was explained by reactions of two first generation RO_2 radicals ($C_{18}H_{26}O_{5-10}$), one first and one second generation RO_2 ($C_{18}H_{28}O_{9-12}$) or two second generation RO_2 resulting in the dimer $C_{18}H_{30}O_{11}$. Although dimers have in general lower O:C ratios than monomers, they are expected to be less volatile due to higher molecular weight and more functional groups making them candidates to participate in nucleation processes (Kirkby et al., 2016).

Organonitrates (ON) are formed as soon as sufficient NO_x is present in the atmosphere. ON are highly important for the reactive nitrogen budget wherein the formation of highly functionalized organic nitrates can contribute significantly to secondary organic aerosol (Lee et al., 2016; Bianchi et al., 2017). In this study we refer to compounds that only consist of H, C and O as HOM monomers or HOM dimers and to N containing compounds as ONs.

NO_x influences the oxidation of organics directly by changing oxidant levels (reducing or increasing OH, depending on the NO_x regime) and indirectly by influencing RO_2 chemistry. In high NO_x environment such as urban areas the reaction of NO with RO_2 radicals [can compete with the autoxidation mechanism \(reaction 1 and 2\) and thus potentially inhibit HOM while favouring ON formation \(reaction 1\)](#).



~~can compete with the autoxidation mechanism (reaction 1 and 2), and thus potentially inhibit HOM while favouring ON formation (reaction 1).~~ Although ON may have high O:C they differ from HOM as they contain at least one nitrogen atom. While HOM formation from BVOCs has been intensively studied, only few studies have been conducted focusing on the formation of HOM from anthropogenic aromatic volatile organic compounds (AVOCs) (Molteni et al., 2018; Wang et al., 2017). However, these studies indicate that AVOCs have a strong potential to form HOM under NO_x free conditions and proposed that they may play a crucial role in NPF and particle growth of SOA in urban areas. Regarding SOA yields a number of smog chamber studies have been conducted in order to investigate the oxidation of TMB with OH radical under different NO_x and aerosol seed conditions (Paulsen et al., 2005; Rodigast et al., 2017; Wyche et al., 2009; Huang et al., 2015; Sato et al., 2012). They reported that under higher NO_x:VOC conditions, SOA yield is reduced compared to medium or lower NO_x:VOC conditions. The NO_x:VOC, in almost all studies, was < 1, apart from one experiment (Wyche et al., 2009), with NO_x:VOC = 1.9 in which the SOA yield was 0.29, compared to yields up to 7.47 under lower NO_x conditions.

In this study we investigate the oxidation of TMB in a laminar flow reactor, while different NO_x and OH conditions were applied. A nitrate chemical ionization atmospheric pressure interface time of flight mass spectrometer (CI-APi-TOF-MS) (Junninen et al., 2010; Jokinen et al., 2012) was used to monitor the oxidation product distribution. We show the formation of HOM and nitrate containing compounds with and without NO_x added to the reaction system. Possible mechanisms leading to the formation of ON and suppression of particle formation are discussed.

2 Materials and Methods

The measured HOM were generated using the laminar flow Gothenburg Potential Aerosol Mass reactor (Go:PAM), initially described by Watne et al. (Watne et al., 2018). The Go:PAM is a 100 cm long, 9.6 cm wide quartz glass cylinder which is irradiated over a length of 84 cm by two 30 W Phillips TUV lamps (254 nm); a schematic is shown in Figure 1. The OH radicals are produced inside Go:PAM by photolysing O₃ in the presence of water vapour. The O₃ is generated outside Go:PAM by photolyzing pure O₂ (UVP Pen-Ray® Mercury Lamps, 185 nm) and distributed in 3 L min⁻¹ particle free and humidified air (Milli – Q) over the reactor cross section. The VOC was introduced through a gravimetrically characterized diffusion source (see [SI-Figure S24](#)) centrally at the top of the reactor with a flow of 8 L min⁻¹ ~~while NO was introduced via a NO gas cylinder.~~ Flows were adjusted for a median residence time of 34 s in Go:PAM. A funnel shaped device is subsampling the centre part of the laminar flow to minimize wall effects on the sample. A condensation particle counter (CPC, 3775 TSI) was used to measure the number particle concentration in the sample flow. O₃ was monitored by a model 202 monitor (2B Technologies), relative humidity by a Vaisala HMP60 probe and NO_x by a model 42i monitor (Thermo Scientific) over the course of the experiments. The OH exposure, over the residence time in the reactor, for NO_x free conditions without added TMB was measured using SO₂ titration (Teledyne T100) as described by Kang et al. (Kang et al., 2007). [Gas phase O₃ oxidation](#) products were measured with an Atmospheric Pressure interface High Resolution Time of Flight Mass Spectrometer (APi-TOF-MS, Aerodyne Research Inc. & Tofwerk AG) (Junninen et al., 2010; Jokinen et al., 2012) in connection with a A70 CI-inlet (Airmodus Ltd) (Eisele and Tanner, 1993). The CI inlet is a laminar flow inlet operated with a sheath flow of 20 L min⁻¹ containing NO₃⁻ ions which are generated by ionizing HNO₃ using an ²⁴¹Am foil upstream in the inlet design. The sample stream from Go:PAM is introduced in the centre of the sheath flow at a rate of 8 L min⁻¹. The NO₃⁻ ions are electrostatically pushed into the sample flow and form stable adducts with sample molecules as described by Ehn et al. (2012). The reaction time of oxidation products and NO₃⁻ is a few hundred ms before being subsampled

into the TOF-MS at 0.8 L min^{-1} by a critical orifice. Differential pumping decreased the pressure from 103 mbar in the CI source to 10^{-6} mbar in the TOF extraction region where HOM are detected as negatively charged clusters with NO_3^- .

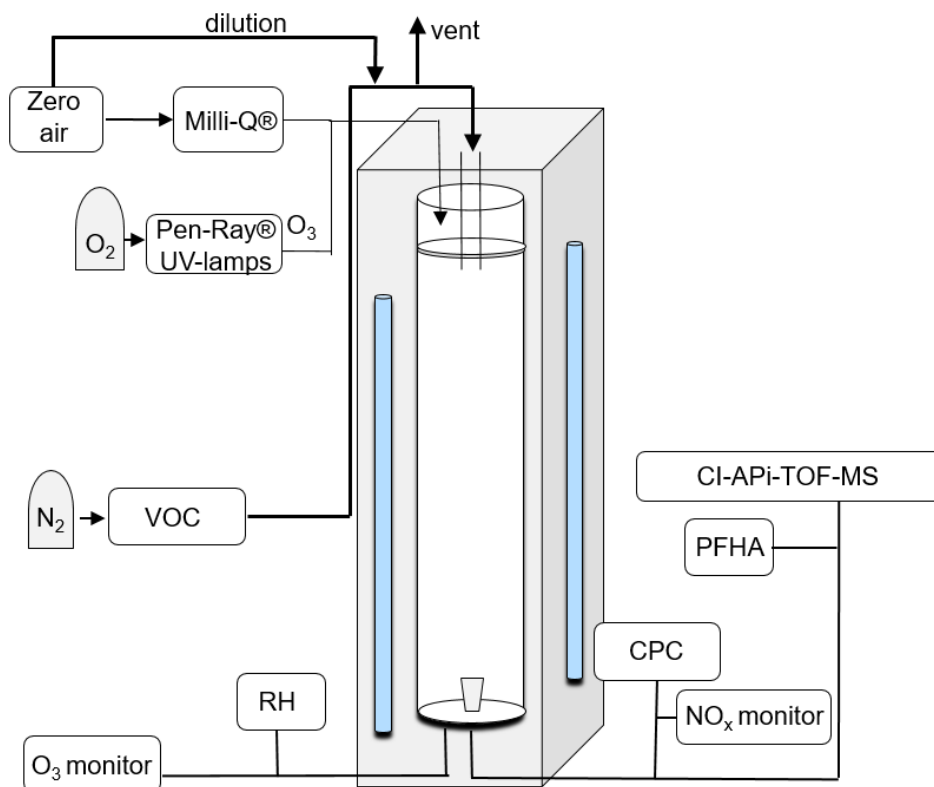


Figure 1: Schematics of the experimental setup with Go:PAM chamber connected to CI- API-TOF-MS.

A kinetic box model was used to simulate the chemistry in the Go:PAM reactor. The core of the model were first described by Watne et al. (Watne et al., 2018). The model consists of 32 species and 68 reactions now including TMB chemistry partly from the MCM v3.3.1 (Jenkin et al., 2003) as well as proposed mechanisms and rate coefficients for NO_2 chemistry (Atkinson et al., 1992; Finlayson-Pitts, 1999) and highly oxygenated compounds (Ehn et al., 2014; Berndt et al., 2018; Zhao et al., 2018) (see SI [Table S24](#)). The photon flux used in the simulations was tuned to match measured decay of O_3 while an OH sink was added to match the observed OH exposure in the background experiment, i.e. without the addition of TMB. The model was run for all experiments with and without NO_x . Primarily, the modelled output on OH exposure for each experiments was used to interpret the results and for calculating the consumed TMB. However, broadly the modelling output was also used to understand the effects of changing experimental conditions on monomer, dimer and organo-nitrate (ON) production. The experiments without NO_x were named 1-4 denoting the increase in OH exposure and experiments with NO_x were denoted according to their $\text{NO}_x / \Delta\text{TMB}$ and high (H) and low (L) OH exposure as seen in Table 1.

3 Results and Discussions

Table 1 summarises eight experiments where TMB has been oxidised by various amounts of OH using the Go:PAM unit. Generally, a high OH production, induced either by increased light exposure (two lamps) or elevated ozone concentration, resulted in new particles (e.g. exp 3 and 4) while addition

of NO_x reduced or suppressed the particle formation. The results from the kinetic model show that the amount of reacted TMB ranges from 5 – 30 ppb, depending on OH exposure (SI Figure S1). An overview of the oxidation product distribution measured with the CI- API-TOF-MS for different conditions is shown in Figure 3 and Figure 4. The compounds were detected as nitrate clusters at $m/z = \text{mass}_{\text{compound}} + 62$. The spectra in Figure 2-3 and 3-4 show significant ion signals from oxygenated hydrocarbons retaining the 9 carbons from the original TMB with either even H numbers (closed shell) or odd H numbers (open shell) with limited amount of products from fragmentation, i.e. ions with less than nine C. C₉ compounds with an O/C ratio of 6/9 or higher were classified as HOM monomers with the general formula C₉H₁₂₋₁₆O₆₋₁₁ in the mass range 280 – 360 m/z . Oxygenated hydrocarbons found in the range 460 – 560 m/z containing 18 C were classified as dimers with chemical formulas C₁₈H₂₄₋₃₀O₁₀₋₁₆. The monomer with the highest intensity detected was C₉H₁₄O₇ m/z 296. The highest intensities among the dimers were C₁₈H₂₆O₁₀, C₁₈H₂₈O₁₁ and C₁₈H₂₈O₁₂ at m/z 464, m/z 482 and m/z 498, respectively. In addition to HOM monomers and dimers, nitrogen containing compounds were found as C₉ compounds with one or two N or C₁₈ compounds with one N. The nitrogen containing compounds were of the general formulas C₉H₁₂₋₁₈NO₆₋₁₃, C₉H₁₂₋₁₈N₂O₈₋₁₅ and C₁₈H₁₈₋₂₄NO₆₋₁₀. The dominating ON were C₉H₁₃NO₈ at m/z 325, C₉H₁₅NO₁₀ at m/z 359 and C₉H₁₄N₂O₁₀ at m/z 372 respectively. In the experiments where NO_x was added, the formation of ON compounds was increasing with the NO_x concentration. In parallel, the levels of HOM monomers and dimers were reduced with NO_x concentration, where dimers were stronger affected than monomers. Even if the fragmentation products were limited some fragmentation leading to less than 9 carbons could be observed. The most prominent fragments were assigned molecular formulas C₄H₇NO₇ at m/z 243, C₄H₆O₁₂ at m/z 246, C₅H₆O₁₂ at m/z 285 and C₆H₉NO₇ at m/z 269. Some compounds with C numbers of 15 and 17 were detected in the range 270 – 560 m/z but their contribution to the total signal was negligible (Figure 3 Figure 2).

Table 1: Experimental conditions for experiments with 30 ppb TMB. Ozone and initial NO_x concentration at time 0 are given in ppb and explicitly modelled OH exposure in molecules s cm⁻³. TMB reacted (Δ TMB) in ppb after a reaction time of 34 s and particle number concentration given in # cm⁻³ after reaching steady state in Go:PAM. RH in all experiments was 38%.

#	[O ₃] ₀	[NO _x] ₀	OH exposure	Δ TMB	NO _x / Δ TMB	Particle number	Contribution of top 10 species (%)
1	~19	5	3.5×10 ⁹	5.4	0.9	-	28.6
2	~19	5	7.1×10 ⁹	9.9	0.5	-	29.8
3	~100	3	3.8×10 ¹⁰	26	0.1	60 ± 14	38.6
4	~100	3	2.1×10 ¹¹	30	0.1	1610 ± 217	35.9
NO _x 9	~9	82	6.3×10 ⁹	9	9.1	-	52.4
NO _x 3 _L	~12	38	7.9×10 ⁹	11	3.5	-	42.3
NO _x 3 _H	~100	79	3.1×10 ¹⁰	25	3.2	-	34.2
NO _x 1	~100	35	9.1×10 ¹⁰	30	1.2	170 ± 50	30.5

The relative contribution of the different compound classes to the total assigned signal are shown in Figure 2. It is apparent that HOM monomers and dimers dominate in the experiments with low NO_x. The contribution of the monomers to the total oxidation product signal ranges from 20.7- 42.1% and dimers make 6.8 – 43.3 % of the total, depending on experimental conditions. Dimer contributions are highest at high OH exposure (exp 3 and 4 with estimated OH exposure of 3.8×10¹⁰ and 2.1×10¹¹ molecules s cm⁻³, respectively) and decrease with increasing NO_x. Nitrated compounds dominated the spectra with contributions up to ~75% in the experiments with highest amount of NO_x. Surprisingly,

some nitrated compounds were also found in the experiments without added NO_x which may stem from background NO contamination (~3-5ppb).

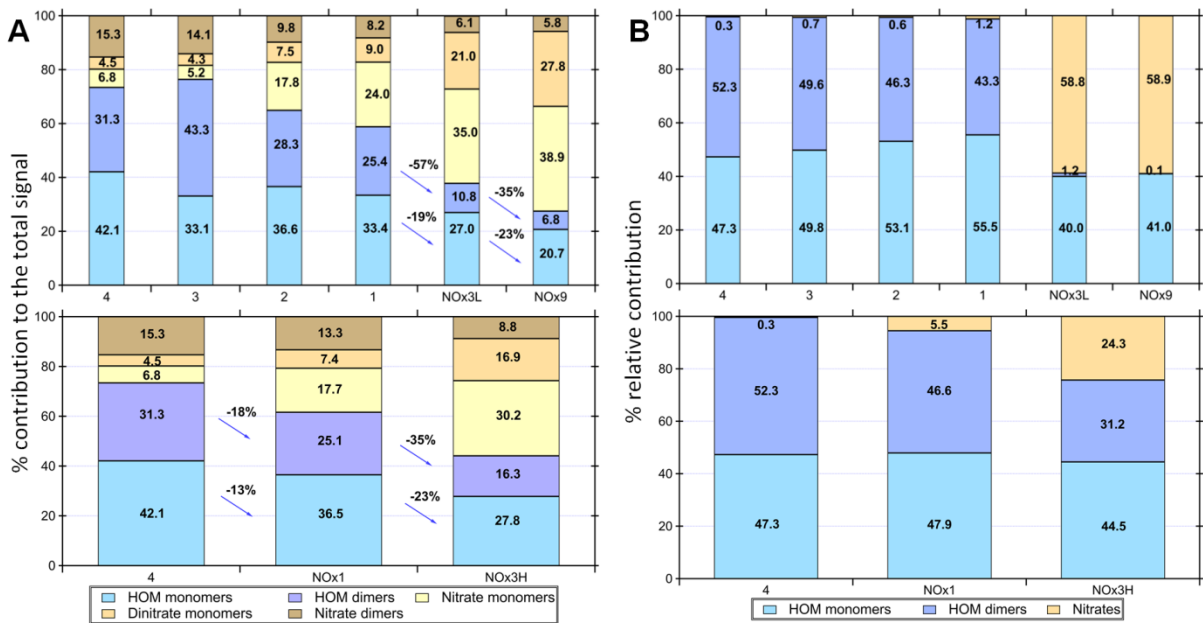
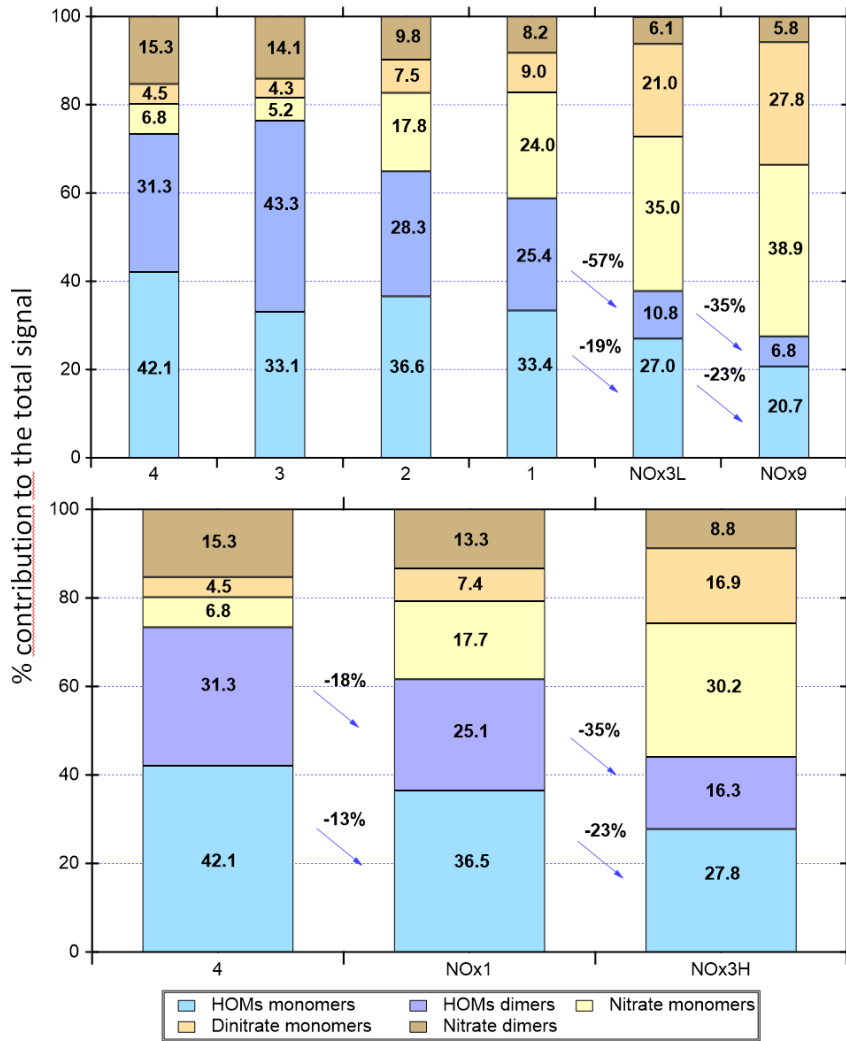


Figure 2: A) Overview of different compound groups to the total explained signal. ~~The influence of increased NO_x/VOC on the product distribution.~~ Top panel illustrates the influence of a decrease of OH exposure (exp 4 - exp 1) and further decrease after adding NO_x in exp NO_x3L – exp NO_x9. Dimers show a larger relative reduction than monomers with increasing NO_x/VOC. Bottom panel shows the influence of increased NO_x/VOC on the product distribution. Experiments 4, 3 and NO_x1 resulted in particle formation. B) Modelled product distribution shown as lumped categories of nitrated compounds, HOM monomers and dimers and their relative contributions.

Recently, Molteni et al. (2018) assigned 17 compounds making up 80% of the total detected signal for HOM oxidation products from the reaction of TMB with OH. Their compound with the highest fraction of the signal (24.2%) was the dimer C₁₈H₂₆O₈. This compound was not detected in our study. We did neither detected deprotonated compounds in the mass range 270 – 560 *m/z* nor HOM monomers with 17 H nor compounds with O/C<0.55 which were found by Molteni et al. (2018). However, we do find 10 of the previously reported 17 monomers and dimers in our spectra. The oxidation product distributions in our experiments are in general term more diverse, i.e. we found more compounds with smaller yields compared to Molteni et al. (2018). In our experiments the highest 20 compounds together explain 46 – 63 % of the total signal with the individual highest oxidation products contributing only between 4.4 and 16%. These differences can be the result of different experimental conditions and set up. In our study the residence time is almost double compared to Molteni et al., leading to the formation of more oxidized compounds, especially more oxidized dimers, which have been reported in this study. In addition we produce OH radicals in the full length of the flow reactor enhancing the effects of secondary chemistry. Despite these differences there is a general agreement on the conclusions for the NO_x free conditions with the Molteni et al. study where one rapidly form HOM of very low volatility, that can initiate NPF.

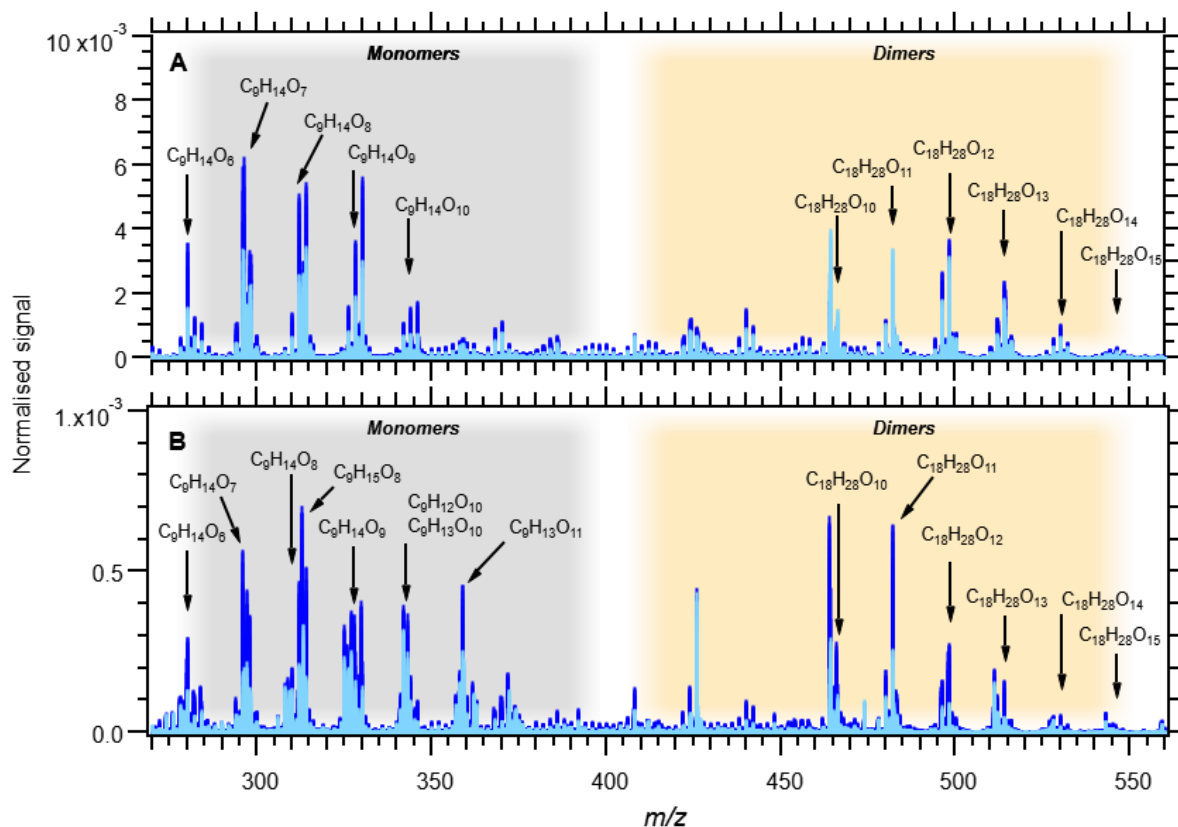


Figure 3: Mass spectra of all experiments without NO_x: 1, 2, 3, and 4. Panel A shows experiments 3 (light blue) and 4 (blue) with OH exposure of 2.87×10^{11} and 3.47×10^{11} molecules $s^{-1} cm^{-3}$ respectively. Panel B shows experiment 1 (light blue) and 2 (blue) with of 3.47×10^{10} and 7.62×10^{10} molecules $s^{-1} cm^{-3}$ respectively. The signal at m/z 426 is associated with the used mass calibrant PFHA. Note the ten times lower Normalised Signal scale in B.

The amount of TMB reacted after 34 s in the experiments ranges from 30 ppb (almost all) in experiment 4 to 5 ppb in experiments 1 and NO_x9 (comp. Table 1 and Figure S1). The signal intensities of the HOM monomers are increasing with increasing OH exposure. Dimer compounds also increase with increasing OH and reach their highest levels in exp 3, resulting in the highest ratio of dimer to monomer (see Figure 2). Faster conversion of TMB will result in higher initial RO₂ levels enabling faster RO₂ + RO₂ (self-) reaction. The concentration profile of RO₂ in exp 1 and 2 is lower and more evenly spread out over the length of Go:PAM (Figure S1) and the influence of the RO₂ + RO₂ reaction will be less in these experiments compared to exp 3 and 4. Enhanced OH exposure does not only affect the monomer/dimer ratio but also the total amount of compounds measured. Observed compounds were 10 times higher in the high OH exposure exp 3, 4, compared to exp 1, 2. This was also valid for the experiments with added NO_x (NO_x1 and NO_x3_H vs NO_x3_L and NO_x9). Under high OH exposure (exp 4) the major HOM monomer is C₉H₁₄O₇ with a contribution of 5.5 % to the total explained signal, followed by C₉H₁₆O₉ and C₉H₁₄O₈, contributing 4.6 and 4.5 % respectively.

At the lowest OH exposure (exp 1) the major signals comprise the monomer C₉H₁₂O₁₀ and the dimers C₁₈H₂₆O₁₀ and C₁₈H₂₈O₁₁, contributing 4.4, 4.0 and 3.4 % to the total. These dimer compounds, C₁₈H₂₆O₁₀ and C₁₈H₂₈O₁₁, are the highest signals in exp 2 and 3. Two open shell species were found among the larger signals in exp 1 and 2 (see [Figure 2](#)[Figure 3](#)): C₉H₁₅O₈ and C₉H₁₅O₇.

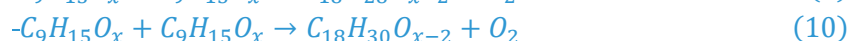
The number of H atoms is a characteristic for HOM monomers and dimers. An overview of different oxidation product generations is given in Table 2. We observe HOM monomers with 12-16 H and all compounds with an even number of H are closed shell products. Compounds with an uneven number of H are open shell molecules (radicals). Following the proposed termination scheme by Mentel et al. (2015) compounds with 12 H can be identified as first generation monomers (terminated from $C_9H_{13}O_x$ radicals, [reaction 3](#)) and compounds with 16 H as second generation monomers (terminated from $C_9H_{15}O_x$ radicals, [reaction 4](#)). $C_9H_{14}O_x$ can [be either first or second generation products and](#) originate from either $C_9H_{13}O_x$ or $C_9H_{15}O_x$ ([reactions 5 and 6](#)).



The RO_2 radicals $C_9H_{13,15}O_x$ can form dimers likely via the reaction



Such reaction is possible between any HOM- RO_2 , first or second generation (and other C_9 peroxy radicals with sufficient high abundance). Two first generation HOM- RO_2 will result in $C_{18}H_{26}O_x$ dimers ([reaction 8](#)) while one first and one second generation HOM- RO_2 produce a $C_{18}H_{28}O_x$ ([reaction 9](#)) and dimerization of two second generation HOM- RO_2 will result in dimers of the formula $C_{18}H_{30}O_x$ ([reaction 10](#)).



A closer examination of the contribution of different HOM generations in Table 2 shows that first generation monomers with 12 H are showing the highest contribution in experiments with low OH exposure (exp 1, 2) while monomers with 14 H gain importance with higher OH exposure. The second generation monomers with 16 H dominate in experiments with the highest OH exposure (exp 3, 4). The dimer population with 28 H has a larger fraction of the total signal at higher OH exposures compared to dimers with 26 H. Dimer population with 30 H is generally lower than other dimers but has the highest fraction in exp 4. The overall dimer fraction of up to 43% in this study (Figure 2) is similar to the dimer fraction of 40% reported by Molteni et al. (2018). However the relative contributions of monomer and dimer generations differ. We find higher contributions of H_{12} monomers (up to 11%) and a higher contribution of H_{28} dimer (up to 12%) under our experimental conditions. The contribution of H_{14} monomers and H_{26} dimers is significantly less compared to Molteni et al. (2018).

Increasing OH exposure promotes second OH attacks on oxidation products leading to the observed reduction of first generation products ($C_9H_{12}O_x$) as well as increase of second generation products ($C_9H_{14}O_x$ and $C_9H_{16}O_x$). [The \$C_9H_{14}O_x\$ products have mainly characteristics of second generation products, as their contribution is enhanced in the experiments with higher OH exposures \(Table S1\), in which there is an enhanced possibility for secondary chemistry initiated by reaction of OH with the first generation products.](#) The increased oxidation degree can also explain the formation of dimers ($C_{18}H_{28}O_x$) from first and second generation RO_2 ($C_9H_{13}O_x$ and $C_9H_{15}O_x$) at higher OH exposure and the increase in second generation dimers (~~$C_9H_{15}O_x + C_9H_{15}O_x \rightarrow C_{18}H_{30}O_x$~~). Open shell species are

observed as first generation RO₂ (C₉H₁₃O_x) and have a higher contribution lower at OH exposures. Second generation RO₂ (C₉H₁₅O_x) have the highest contribution in exp 3. At the highest OH exposures in exp 4, the contribution of ~~(C₉H₁₅O_x) radicals, one of the top ten contributors to the signal (Table S1), is reduced, while the contribution of the second generation products at the expense of (C₉H₁₄O_x and C₉H₁₆O_x) -HOM and dimers increases.~~

Table 2: Contribution of oxidation product families to the total signal between 270 – 560 m/z

Compound family	1	2	3	4	NO _x 9	NO _x 3 _L	NO _x 3 _H	NO _x 1
C ₉ H ₁₂ O _x	11.3	7.8	3.5	5.4	8.5	9.3	5.9	5.4
C ₉ H ₁₃ O _x	5.7	4.5	3.3	2.1	6.0	7.0	5.6	4.2
C ₉ H ₁₄ O _x	8.3	10.8	9.9	17.4	4.3	6.6	8.0	13.0
C ₉ H ₁₅ O _x	5.6	7.2	9.4	4.1	2.4	3.3	4.6	4.7
C ₉ H ₁₆ O _x	4.8	8.0	7.7	14.5	1.5	2.5	4.8	10.3
C ₁₈ H ₂₆ O _x	8.5	9.1	8.5	9.3	0.8	2.0	2.7	6.0
C ₁₈ H ₂₈ O _x	7.1	9.9	9.3	11.0	0.4	1.2	2.6	6.9
C ₁₈ H ₃₀ O _x	0.7	1.0	2.3	2.6	0.4	0.4	0.9	1.7
C ₉ H ₁₃ NO _x	6.2	4.7	0.6	0.6	26.8	17.1	10.1	4.8
C ₉ H ₁₅ NO _x	6.4	5.6	0.7	0.9	3.7	10.3	14.5	8.5
C ₉ H ₁₄ N ₂ O _x	2.1	1.7	1.0	1.1	18.7	11.8	7.5	1.9

In this study the contribution of C₁₈H₂₈O_x shows that both first and second generation HOM-RO₂ were dimerising. The kinetics of dimer formation, if produced from RO₂ self-reaction, depends on the square of [HOM-RO₂] and their relative importance will increase with the RO₂ concentration. Increased local RO₂ concentrations (in the first part of Go:PAM) would explain the increase of dimers with increasing OH exposure.

Substantial particle formation was observed in exp 4, under the highest OH exposure. Although the amount of reacted TMB in exp 3 and 4 is similar (26 and 30 ppb respectively), significant particle formation was not observed under the conditions of exp 3. The rate at which new particle formation (nucleation) occurs is related to the chemical composition and concentration of the nucleating species (McGraw and Zhang, 2008). After reaching the critical nucleus, particle growth becomes spontaneous in the presence of condensable vapour. Apparently, the local concentration of nucleating species or condensable vapour was not high enough in exp 3 to yield large numbers of particles, compared to exp 4. According to recent studies (Ehn et al., 2014; Trostl et al., 2016; Mohr et al., 2017; McFiggans et al., 2019) dimers play an important role in new particle formation. Mohr et al. (2017) found decreased levels of gas phase dimers in ambient air during NPF events, which is in line with our observations of lower dimer levels in the presence of particles in exp 4, compared to exp 3. A large enough concentration of low volatility dimers obviously helps forming critical nuclei that then grow by condensation. Note that the newly formed particles will provide an additional sink for dimers and thus reduce their presence as observable gas phase products at the end of the flow reactor.

Influence of NO_x

In the experiments NO_x1, NO_x3_H, NO_x3_L and NO_x9, the NO_x levels were increased (Table 1). As already has been described NO_x was introduced to the Go:PAM as NO. After the addition of ozone,

the ozone concentration decreases from 100 ppb to ~80 ppb at the experiment with lower NO_x levels and to ~50 ppb at the experiment with higher NO_x levels, as it reacts with NO producing NO₂. For both high and low NO_x conditions there is NO left after the initial reaction with ozone (see grey areas at of Figure S3). The presence of NO_x gave nitrogen containing C₉ compounds with one or two N atoms and C₁₈ compounds with only one N atom, in addition to HOM monomers and HOM dimers. These compounds are expected to be nitrates or peroxy nitrates, as it is highly unlikely to form nitro-aromatic compounds from TMB (Sato et al., 2012). N-containing compounds were the dominating species in experiments with NO_x (see Figure 2), except for the experiment NOx1 with the smallest amount of NO_x added and a high OH exposure (NOx1). The amount of nitrated compounds increased with the amount of added NO_x at the expense of HOM monomers and HOM dimers as illustrated by the arrows in Figure 2. The effect of the added NO_x is attenuated at higher OH exposure. E.g., the nitrated monomers are reduced from 35.0 and 38.9% at low OH exposure down to 17.7 and 30.2% at high OH exposure. Under elevated NO_x conditions nitrated species were found among the 10 compounds with the highest contribution to the respective total signal, (see the top-ten lists in SI Table S1 and Figure 4).

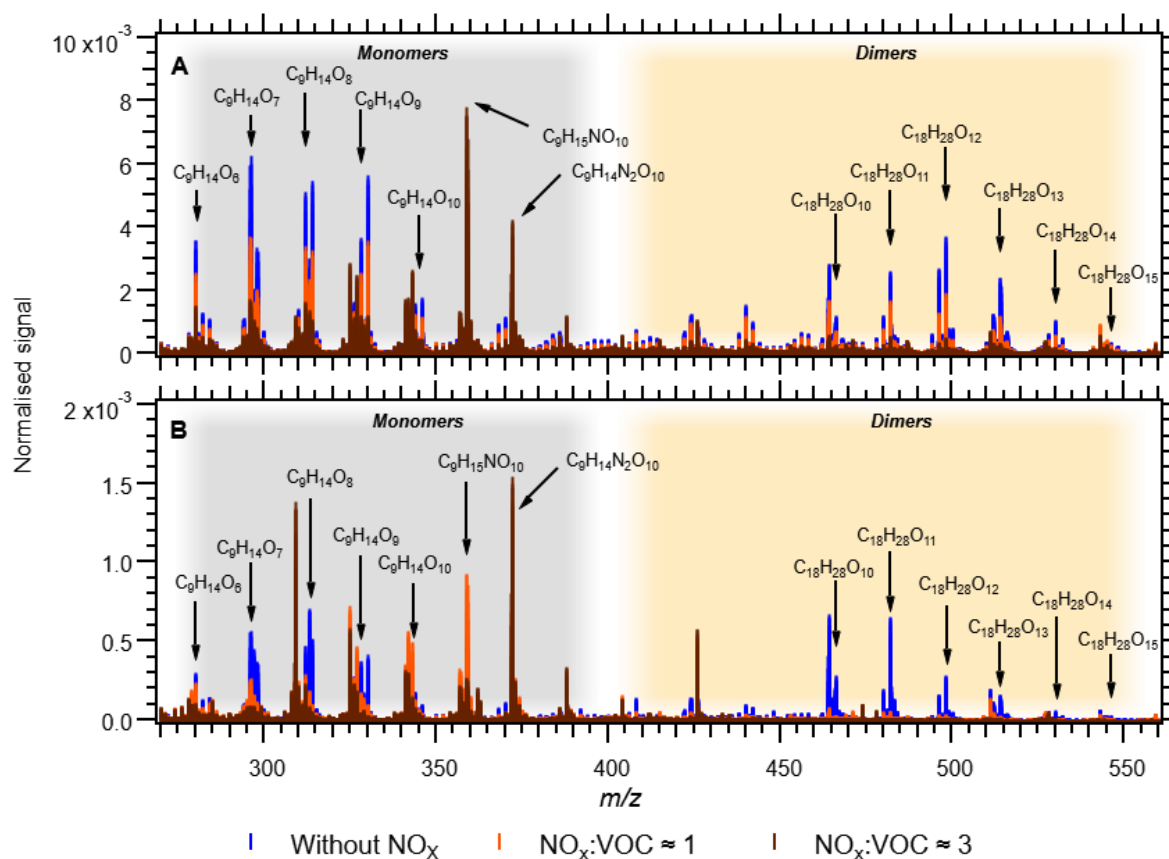


Figure 4: Comparison of mass spectra of HOM and nitrates. Panel A shows experiment 4 (blue), NOx1 (orange) and experiment NOx3_H (brown). Panel B shows experiments 2 (blue), NOx3_L (orange) and NOx9 (brown).

For the two experiments with low OH exposure where the nitrated species dominated, seven out of the top ten species were nitrated with the highest signal arising from the di-nitrated compound (C₉H₁₄N₂O₁₀). In these two experiments the top-ten compounds contributed the most to the observed signal (42.3 and 52.4%); most likely owing to the high fraction of nitrated species acting as radical chain termination products. Under highest NO_x conditions, the high OH exposure experiment (NOx3_H) has six nitrated compounds in the top-ten list with the di-nitrated C₉H₁₄N₂O₁₀ on the second rank. In

experiment NOx1 only one nitrated species (C₉H₁₅NO₁₀) is found in the top-ten list despite the elevated NO_x conditions.

Dimer formation is drastically reduced in the presence of elevated NO_x. The NO_x effect on NPF was clear and high NO_x/ΔTMB suppresses NPF from TMB oxidation, a trend that was also observed by Wildt et al. (2014) and Lehtipalo et al. (2018) for NPF from monoterpene oxidation. Whenever the products were dominated by ON (NOx3_L, NOx9 and NOx3_H) particle formation was not observed. Reduced particle formation was observed in NOx1 compared to exp 1 which had a higher contribution of HOM. Owing to the importance of dimers for NPF, as reported by Lehtipalo et al. (2018), we suggest that the reaction of RO₂ + NO resulting in ON is responsible for the observed reduced particle formation, because it competes with the dimer formation from RO₂ + RO₂. This reaction is also reducing the contribution of HOM monomers and dimers with increasing NO_x/ΔTMB and decreasing OH exposure from a total of 61% in exp NOx1 (OH exposure=9.1×10¹⁰ molecules s cm⁻³) to 27.5% in NOx9 (OH exposure=6.3×10⁹ molecules s cm⁻³). The reaction RO₂ + NO reduce the amount of HOM monomers and dimers in competing with autoxidation and termination by RO₂+RO₂ or RO₂+HO₂. The yield of ON from NO+RO₂ ~~must-might~~ be high ~~or maybe close to unity~~ based on the measurable increase of ON- and the decrease of NO_x in the system (see ~~Figure 7~~Figure S3).

The contribution of HOM monomer generations follows the general trend observed in experiments without NO_x. The first generation HOM have higher contribution at low OH exposures in NOx3_L and NOx9 and the contribution of second generation HOM is higher the higher the OH exposure is. Similarly, the contribution of C₉H₁₄O_x is increasing with increasing OH exposure. Analogously to the families of HOM, different families of nitrates can be defined. Table 2 gives an overview of the nitrate families and how they contribute to the total signal in the experiments. At lowest OH exposures we find the highest contributions of first generation nitrates (C₉H₁₃NO_x) as well as di-nitrates (C₉H₁₄N₂O_x). The contribution of second generation nitrates (C₉H₁₅NO_x) is increasing with increasing OH exposure and is highest in NOx3_H.

For the formation of observed first generation nitrates C₉H₁₃NO₆₋₁₂ (C₉H₁₃NO_x in Table 2) we propose the reaction of a first generation (HOM-)RO₂ with NO following the pathway:



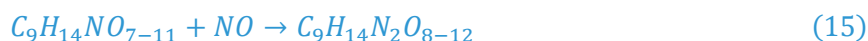
The precursor C₉H₁₃O₅ is formed after ~~two-one~~ autoxidation steps and its termination reaction with NO results in C₉H₁₃NO₆ which has only minor contribution. C₉H₁₃NO_{7&8}, with higher contribution in exp NOx3_L and NOx9 can be formed from the radicals C₉H₁₃O₆ and C₉H₁₃O₇ respectively. The even oxygen number in C₉H₁₃O₆ indicates that the compound should have undergone a transformation to RO (via reaction with RO₂ or NO) and subsequent H-shift and further O₂ addition (Vereecken and Peeters, 2010;Mentel et al., 2015). [A proposed detailed reaction mechanism is depicted in Figure 5.](#)

Second generation nitrates (C₉H₁₅NO₈₋₁₂) can be formed after an additional OH attack (and introduction of an additional H) on a first generation (HOM) monomer, which explains the increase of these compounds with increasing OH exposure. The termination of the RO₂ radical chain with NO (reaction ~~5~~12) will then lead to the formation of the second generation nitrate. The formation of RO₂ precursor species with ~~lower~~7-8 O numbers, i.e. C₉H₁₅O₇₋₈ likely stem from compounds terminated earlier in the radical chain process (C₉H₁₄O₄₋₅), which do not fall in the typical HOM class (O₂:C ≥ 6₂:9). The reaction of a first generation nitrate with OH, followed by autoxidation could also possibly produce C₉H₁₅NO₈₋₁₂ by terminating via ~~hydroxyl-peroxy~~ (reaction ~~6~~13) or hydroperoxy pathway (reaction ~~7~~14).





For the formation of the most abundant di-nitrates of the formula $C_9H_{14}N_2O_{8-12}$ (reaction 815), OH has to attack a nitrated compound $C_9H_{13}NO_{6-10}$ and the RO_2 radical chain has to be terminated with NO (Figure 5):



The precursor species $C_9H_{14}NO_7$ would be in this case formed from the OH attack on the smallest possible nitrate $C_9H_{13}NO_4$ (formed after one autoxidation step and NO termination).

It should be noted that the formation of peroxy nitrates via the reaction $RO_2 + NO_2 \rightarrow RO_2NO_2$ with alkyl and acyl- RO_2 (PAN-like) cannot be ruled out as a potential formation mechanisms of nitrates.

The volatility of the produced ON seems to be too high (compared to dimers) to initiate NPF at the present concentrations as seen from the reduction in particle formation potential from exp 4 (HOM dominated, particle formation) to NOx1 (reduction in HOM and increase in ON, reduced particle formation) and NOx3H (ON dominated, no particle formation).

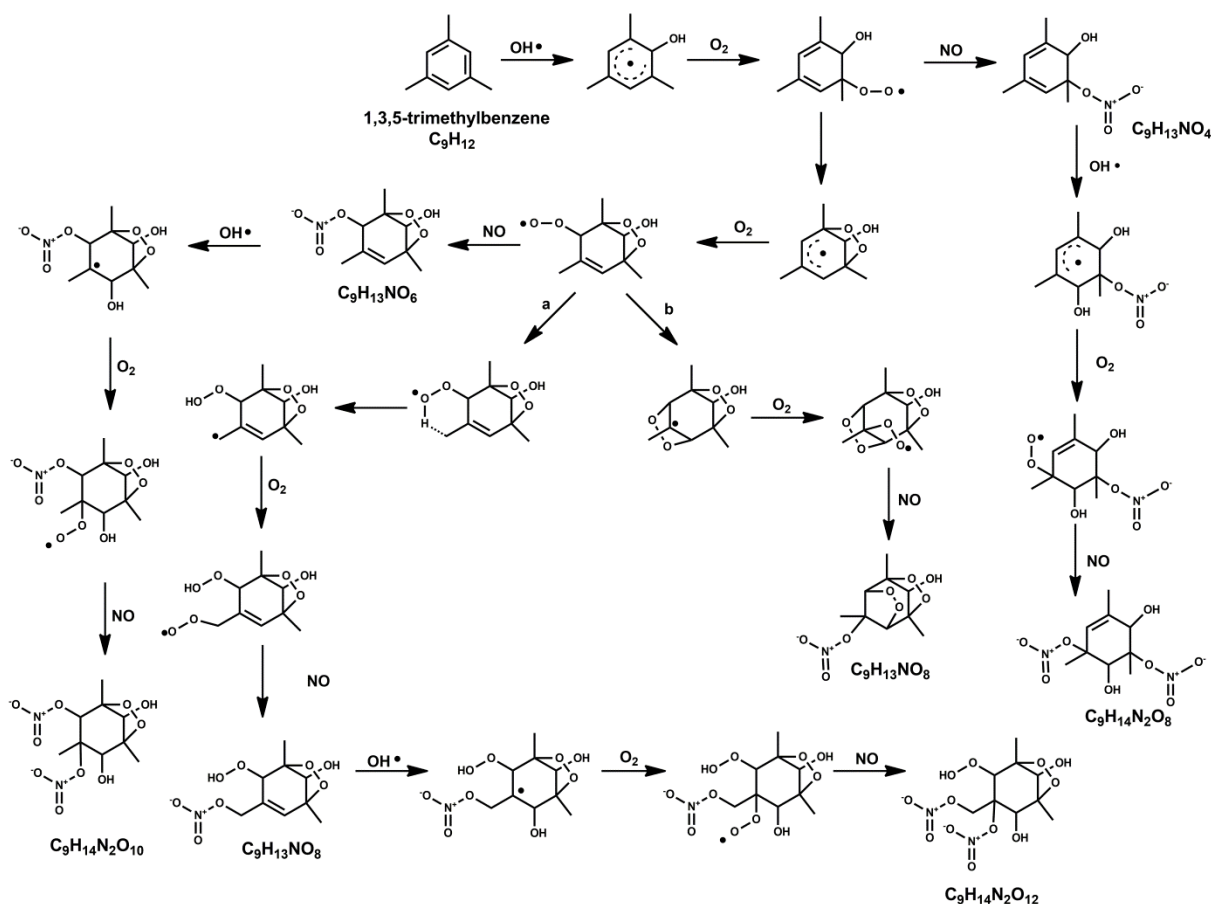


Figure 5: The proposed radical reaction mechanism for the formation of some of the mono- and di-nitrates from TMB mentioned in this study. Two separate mechanisms were suggested for the

[species with the formula C₉H₁₃NO₈, which formation pathways are based on \(a\) \(Wang et al., 2017\) and \(b\) \(Molteni et al., 2018\).](#)

~~Figure 5~~[Figure 2B](#) shows the results for the evolution of HOM monomer, HOM Dimers and organic nitrates (ON) as calculated using the kinetic model described in detailed in SI. The model used has a very simplified scheme for TMB oxidation and subsequent RO₂ chemistry. We implemented a few rate coefficients suggested in the literature in order to demonstrate how those compare with our experimental results. Rate coefficients for RO₂ termination reactions from MCM in combination with rate coefficients of dimer formation by Berndt et al. (2018) (case 1 and 2 in SI [Table S2+](#)) led to an overestimation of dimer compounds. Better representation of the observations were achieved by applying a) the rate coefficients proposed by (Zhao et al., 2018)~~Zhang et al. (2018)~~ for dimer formation ($2.0 \times 10^{-12} \text{ cm}^3 \text{ molecules}^{-1} \text{ s}^{-1}$) and $1.0 \times 10^{-12} \text{ cm}^3 \text{ molecules}^{-1} \text{ s}^{-1}$ for termination and RO formation with branching ratios of 0.4 and 0.6, respectively; b) the rate coefficient ($1.0 \times 10^{-11} \text{ cm}^3 \text{ molecules}^{-1} \text{ s}^{-1}$) from Berndt et al. (2018) for ~~ON formation from~~ HOMRO₂ + NO [with a branching ratio of 0.3 for](#) ($1.0 \times 10^{-11} \text{ cm}^3 \text{ molecules}^{-1} \text{ s}^{-1}$), ~~ON formation (branching ratio 0.3 for reaction 56 in Table S2).~~

In ~~Figure 5~~[Figure 2B](#), the calculated HOM dimer contribution are the sum of medium (produced from HOM-RO₂+RO₂), and highly oxidised dimers (produced from HOM-RO₂ + HOM-RO₂) while the ON includes both organic nitrates (produced from ~~NO+HOM-RO₂+NO~~) and peroxy nitrates (produced from HOM-RO₂+NO₂). The increased production of monomers calculated for exp 1 and 2 is in agreement with experimental results, where we observed a slightly larger contribution from monomers compared to dimers. Calculated concentrations for dimers are ~~similar-higher~~ in exp 3 and [higher in exp 4](#), compared to monomers. Secondary chemistry (reaction of OH with the products and possible formation of a second generation of HOM or nitrates) was not taken into consideration in the model. For the experiment with NO_x (~~Figure 5~~[Figure 2B](#), right panels) the modeled product distribution follows the general trend of monomer, dimer and nitrate that we observe in the exp NOx3_L and NOx9 with a general higher nitrate production compared to monomers and dimers. For the NO_x experiments with high initial ozone, the model can reproduce the higher HOM monomer and dimer levels in NOx1 but slightly overestimates the contribution of dimers. Particle formation was observed in NOx1 which might explain the overestimation owing to missing condensation sink in the model. Modelling NOx3_H gives an overestimation of monomers and dimers.

In NOx3_H modelled dimers start forming after ~15 sec. Almost all NO is converted to ON or NO₂ at this point and the reaction HOM-RO₂+NO does not produce additional ON and the modelled levels of ON reach a plateau while contribution of HOM dimers can increase. For exp NOx1 and NOx3_H the model is in better agreement with the measurements if only the HOM - dimer formation (from HOM-RO₂+HOM-RO₂) is taken into account, i.e. highly oxidized dimers excluding medium oxidized dimer (from HOM-RO₂ + RO₂). Generally, the simplified model was able to support our analysis of the TMB chemistry as described above. Furthermore, it gave some support to the recently suggested mechanisms included in case 3 (e.g. ~~(Zhao et al., 2018)~~[Zhang et al. \(2018\)](#))

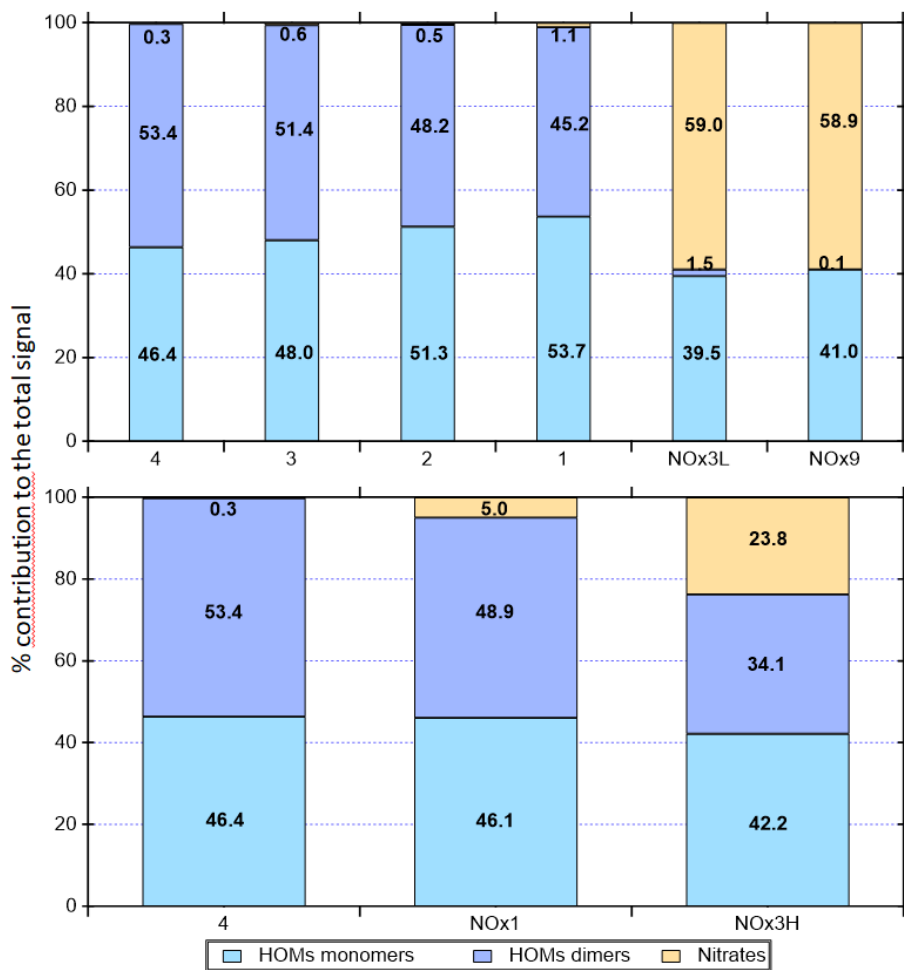


Figure 5: Modelled product distribution to the total for all 8 experiments (compare Fig. 2).

4 Atmospheric implication and Conclusion

We have measured the formation of HOM monomers and dimers from OH initiated oxidation of TMB. The experiments with highest OH exposures lead to particle formation when NO_x was not added. With increasing OH exposure and increased likelihood of a second OH attack, we observe a higher contribution from second generation oxidation products and dimers in general. The latter is attributed to the increased RO_2 concentrations from the increased/fast TMB consumption by OH. The observed products in this study match what would be expected as termination products from previously proposed reaction mechanisms for HOM formation.

The addition of NO_x to simulate urban condition leads to the formation of ON in addition to HOM and a reduction in particle formation potential. We observe that the formation of ON is increasing with increasing $\text{NO}_x/\Delta\text{TMB}$, mostly at the expense of dimers. The presence of ONs, formed at the expense of dimers, can explain the decreased tendency for particle formation. We therefore suggest that the reaction $\text{HOM-RO}_2+\text{NO}$ competes with HOM-RO_2 self-reaction yielding primarily a reduction in dimer formation, which is responsible for the reduction in particle formation. [The experimental designed using the Go:PAM with concentrations of HOx \(and ROx\) higher than ambient would attenuate the influence of added \$\text{NO}_x\$. This will further emphasis the implication of our findings and most likely the \$\text{NO}_x\$ effect would be even more important in the urban atmosphere.](#)

According to studies by (Molteni et al., 2018) and (Wang et al., 2017) [Wang et al. \(2018\)](#) HOM formation from AVOCs was observed and consequently AVOC-HOM were suggested as potential contributors to observed NPF in urban atmospheres. In our study, under NO_x free conditions, we found several of previous identified HOM even if we did not fully agree with the identity and relative importance of all HOM. However, the oxidation in polluted environments will happen under elevated NO_x levels and, as has been shown here this can lead to formation of ON instead of HOM and subsequently a reduction in NPF potential. We conclude that for interpretation of NPF from aromatics in urban areas care should be taken and the OH exposure, NO_x levels and RO₂ concentrations need to be considered in details since they will largely determine if the HOM-RO₂+NO can compete with reactions yielding HOM, and especially HOM dimers.

Data availability: The data set is available upon request by contacting Mattias Hallquist (hallq@chem.gu.se).

Competing Interests: The authors declare that they have no conflict of interest.

Author contribution: [J.H., E.T., T.M. and M.H. designed the experiments. J.H and E.T performed the experiments and data analysis. E.T. performed the modelling. C.M.S. designed the chemical mechanisms. E.T., J.H. and M.H. wrote the paper. All authors commented on the paper and were involved in the scientific interpretation and discussion.](#)

Acknowledgements: The research presented is a contribution to the Swedish strategic research area Modelling the Regional and Global Earth system, MERGE. This work was supported by the Swedish Research Council (grant numbers 2014-05332; 2013-06917) and Formas (grant number 2015-1537).

5. References:

- Atkinson, R., Baulch, D. L., Cox, R. A., Hampson, R. F., Kerr, J. A., and Troe, J.: Evaluated Kinetic and Photochemical Data for Atmospheric Chemistry Supplement-IV - Iupac Subcommittee on Gas Kinetic Data Evaluation for Atmospheric Chemistry, *J Phys Chem Ref Data*, 21, 1125-1568, [Doi 10.1063/1.555918](https://doi.org/10.1063/1.555918), 1992.
- Berndt, T., Richters, S., Jokinen, T., Hyttinen, N., Kurten, T., Otkjaer, R. V., Kjaergaard, H. G., Stratmann, F., Herrmann, H., Sipila, M., Kulmala, M., and Ehn, M.: Hydroxyl radical-induced formation of highly oxidized organic compounds, *Nat Commun*, 7, 13677, [10.1038/ncomms13677](https://doi.org/10.1038/ncomms13677), 2016.
- Bianchi, F., Trostl, J., Junninen, H., Frege, C., Henne, S., Hoyle, C. R., Molteni, U., Herrmann, E., Adamov, A., Bukowiecki, N., Chen, X., Duplissy, J., Gysel, M., Hutterli, M., Kangasluoma, J., Kontkanen, J., Kurten, A., Manninen, H. E., Munch, S., Perakyla, O., Petaja, T., Rondo, L., Williamson, C., Weingartner, E., Curtius, J., Worsnop, D. R., Kulmala, M., Dommen, J., and Baltensperger, U.: New particle formation in the free troposphere: A question of chemistry and timing, *Science*, 352, 1109-1112, [10.1126/science.aad5456](https://doi.org/10.1126/science.aad5456), 2016.
- Bianchi, F., Garmash, O., He, X., Yan, C., Iyer, S., Rosendahl, I., Xu, Z., Rissanen, M. P., Riva, M., Taipale, R., Sarnela, N., Petaja, T., Worsnop, D. R., Kulmala, M., Ehn, M., and Junninen, H.: The role of highly oxygenated molecules (HOMs) in determining the composition of ambient ions in the boreal forest, *Atmos Chem Phys*, 17, 13819-13831, [10.5194/acp-17-13819-2017](https://doi.org/10.5194/acp-17-13819-2017), 2017.
- Bianchi, F., Kurten, T., Riva, M., Mohr, C., Rissanen, M. P., Roldin, P., Berndt, T., Crouse, J. D., Wennberg, P. O., Mentel, T. F., Wildt, J., Junninen, H., Jokinen, T., Kulmala, M., Worsnop, D. R., Thornton, J. A., Donahue, N., Kjaergaard, H. G., and Ehn, M.: Highly Oxygenated Organic Molecules (HOM) from Gas-Phase Autoxidation Involving Peroxy Radicals: A Key Contributor to Atmospheric Aerosol, *Chem Rev*, 119, 3472-3509, [10.1021/acs.chemrev.8b00395](https://doi.org/10.1021/acs.chemrev.8b00395), 2019.
- Chan, C. K., and Yao, X.: Air pollution in mega cities in China, *Atmos Environ*, 42, 1-42, [10.1016/j.atmosenv.2007.09.003](https://doi.org/10.1016/j.atmosenv.2007.09.003), 2008.
- Crouse, J. D., Nielsen, L. B., Jorgensen, S., Kjaergaard, H. G., and Wennberg, P. O.: Autoxidation of Organic Compounds in the Atmosphere, *J Phys Chem Lett*, 4, 3513-3520, [10.1021/jz4019207](https://doi.org/10.1021/jz4019207), 2013.
- Donahue, N. M., Kroll, J. H., Pandis, S. N., and Robinson, A. L.: A two-dimensional volatility basis set – Part 2: Diagnostics of organic-aerosol evolution, *Atmos. Chem. Phys.*, 12, 615-634, [10.5194/acp-12-615-2012](https://doi.org/10.5194/acp-12-615-2012), 2012.

- Ehn, M., Kleist, E., Junninen, H., Petäjä, T., Lönn, G., Schobesberger, S., Dal Maso, M., Trimborn, A., Kulmala, M., Worsnop, D. R., Wahner, A., Wildt, J., and Mentel, T. F.: Gas phase formation of extremely oxidized pinene reaction products in chamber and ambient air, *Atmos Chem Phys*, 12, 5113-5127, 10.5194/acp-12-5113-2012, 2012.
- Ehn, M., Thornton, J. A., Kleist, E., Sipila, M., Junninen, H., Pullinen, I., Springer, M., Rubach, F., Tillmann, R., Lee, B., Lopez-Hilfiker, F., Andres, S., Acir, I.-H., Rissanen, M., Jokinen, T., Schobesberger, S., Kangasluoma, J., Kontkanen, J., Nieminen, T., Kurten, T., Nielsen, L. B., Jorgensen, S., Kjaergaard, H. G., Canagaratna, M., Maso, M. D., Berndt, T., Petaja, T., Wahner, A., Kerminen, V.-M., Kulmala, M., Worsnop, D. R., Wildt, J., and Mentel, T. F.: A large source of low-volatility secondary organic aerosol, *Nature*, 506, 476-479, 10.1038/nature13032, 2014.
- Eisele, F. L., and Tanner, D. J.: Measurement of the gas phase concentration of H₂SO₄ and methane sulfonic acid and estimates of H₂SO₄ production and loss in the atmosphere, *Journal of Geophysical Research: Atmospheres*, 98, 9001-9010, 10.1029/93jd00031, 1993.
- Finlayson-Pitts, B. a. P., J.: *Chemistry of the Upper and Lower Atmosphere*, 1999.
- Gentner, D. R., Jathar, S. H., Gordon, T. D., Bahreini, R., Day, D. A., El Haddad, I., Hayes, P. L., Pieber, S. M., Platt, S. M., de Gouw, J., Goldstein, A. H., Harley, R. A., Jimenez, J. L., Prevot, A. S. H., and Robinson, A. L.: Review of Urban Secondary Organic Aerosol Formation from Gasoline and Diesel Motor Vehicle Emissions, *Environmental science & technology*, 51, 1074-1093, 10.1021/acs.est.6b04509, 2017.
- Guo, S., Hu, M., Zamora, M. L., Peng, J., Shang, D., Zheng, J., Du, Z., Wu, Z., Shao, M., Zeng, L., Molina, M. J., and Zhang, R.: Elucidating severe urban haze formation in China, *Proc Natl Acad Sci U S A*, 111, 17373-17378, 10.1073/pnas.1419604111, 2014.
- Hallquist, M., Wenger, J. C., Baltensperger, U., Rudich, Y., Simpson, D., Claeys, M., Dommen, J., Donahue, N. M., George, C., Goldstein, A. H., Hamilton, J. F., Herrmann, H., Hoffmann, T., Iinuma, Y., Jang, M., Jenkin, M. E., Jimenez, J. L., Kiendler-Scharr, A., Maenhaut, W., McFiggans, G., Mentel, T. F., Monod, A., Prevot, A. S. H., Seinfeld, J. H., Surratt, J. D., Szmigielski, R., and Wildt, J.: The formation, properties and impact of secondary organic aerosol: current and emerging issues, *Atmos. Chem. Phys.*, 9, 5155-5236, 2009.
- Hallquist, M., Munthe, J., Hu, M., Wang, T., Chan, C. K., Gao, J., Boman, J., Guo, S., Hallquist, A. M., Mellqvist, J., Moldanova, J., Pathak, R. K., Pettersson, J. B. C., Pleijel, H., Simpson, D., and Thynell, M.: Photochemical smog in China: scientific challenges and implications for air-quality policies, *National Science Review*, 3, 401-403, 10.1093/nsr/nww080, 2016.
- Hu, M., Guo, S., Peng, J.-f., and Wu, Z.-j.: Insight into characteristics and sources of PM_{2.5} in the Beijing–Tianjin–Hebei region, China, *National Science Review*, 2, 257-258, 10.1093/nsr/nwv003, 2015.
- Huang, M., Lin, Y., Huang, X., Liu, X., Guo, X., Hu, C., Zhao, W., Gu, X., Fang, L., and Zhang, W.: Experimental study of particulate products for aging of 1,3,5-trimethylbenzene secondary organic aerosol, *Atmos Pollut Res*, 6, 209-219, 10.5094/apr.2015.025, 2015.
- Intergovernmental Panel on Climate, C.: *Climate Change 2013 - The Physical Science Basis*, Cambridge University Press, Cambridge, United Kingdom and New York, NY, USA, 1535 pp., 2014.
- Jokinen, T., Sipila, M., Junninen, H., Ehn, M., Lonn, G., Hakala, J., Petaja, T., Mauldin, R. L., Kulmala, M., and Worsnop, D. R.: Atmospheric sulphuric acid and neutral cluster measurements using CI-API-TOF, *Atmos. Chem. Phys.*, 12, 4117-4125, 10.5194/acp-12-4117-2012, 2012.
- Jokinen, T., Sipila, M., Richters, S., Kerminen, V. M., Paasonen, P., Stratmann, F., Worsnop, D., Kulmala, M., Ehn, M., Herrmann, H., and Berndt, T.: Rapid autoxidation forms highly oxidized RO₂ radicals in the atmosphere, *Angewandte Chemie (International ed. in English)*, 53, 14596-14600, 10.1002/anie.201408566, 2014.
- Jokinen, T., Berndt, T., Makkonen, R., Kerminen, V. M., Junninen, H., Paasonen, P., Stratmann, F., Herrmann, H., Guenther, A. B., Worsnop, D. R., Kulmala, M., Ehn, M., and Sipila, M.: Production of extremely low volatile organic compounds from biogenic emissions: Measured yields and atmospheric implications, *Proc. Natl. Acad. Sci. U.S.A.*, 112, 7123-7128, 10.1073/pnas.1423977112, 2015.
- Junninen, H., Ehn, M., Petaja, T., Luosujarvi, L., Kotiaho, T., Kostiaainen, R., Rohner, U., Gonin, M., Fuhrer, K., Kulmala, M., and Worsnop, D. R.: A high-resolution mass spectrometer to measure atmospheric ion composition, *Atmospheric Measurement Techniques*, 3, 1039-1053, 10.5194/amt-3-1039-2010, 2010.
- Kang, E., Root, M. J., Toohey, D. W., and Brune, W. H.: Introducing the concept of Potential Aerosol Mass (PAM), *Atmos. Chem. Phys.*, 7, 5727-5744, DOI 10.5194/acp-7-5727-2007, 2007.
- Kirkby, J., Duplissy, J., Sengupta, K., Frege, C., Gordon, H., Williamson, C., Heinritzi, M., Simon, M., Yan, C., Almeida, J., Trostl, J., Nieminen, T., Ortega, I. K., Wagner, R., Adamov, A., Amorim, A., Bernhammer, A. K., Bianchi, F., Breitenlechner, M., Brilke, S., Chen, X., Craven, J., Dias, A., Ehrhart, S., Flagan, R. C., Franchin, A., Fuchs, C., Guida, R., Hakala, J., Hoyle, C. R., Jokinen, T., Junninen, H., Kangasluoma, J., Kim, J., Krapf, M., Kurten, A., Laaksonen, A., Lehtipalo, K., Makhmutov, V., Mathot, S., Molteni, U., Onnela, A., Perakyla, O., Piel, F., Petaja, T., Praplan, A. P., Pringle, K., Rap, A., Richards, N. A., Riipinen, I., Rissanen, M. P., Rondo, L., Sarnela, N., Schobesberger, S., Scott, C. E., Seinfeld, J. H., Sipila, M., Steiner, G., Stozhkov, Y., Stratmann, F., Tome, A., Virtanen, A., Vogel, A. L., Wagner, A. C., Wagner, P. E., Weingartner, E., Wimmer, D., Winkler, P. M., Ye, P., Zhang, X., Hansel, A., Dommen, J., Donahue, N. M., Worsnop, D. R., Baltensperger, U., Kulmala, M., Carslaw, K. S., and Curtius, J.: Ion-induced nucleation of pure biogenic particles, *Nature*, 533, 521-526, 10.1038/nature17953, 2016.
- Kristensen, K., Watne, Å. K., Hammes, J., Lutz, A., Petäjä, T., Hallquist, M., Bilde, M., and Glasius, M.: High-Molecular Weight Dimer Esters Are Major Products in Aerosols from α -Pinene Ozonolysis and the Boreal Forest, *Environmental Science & Technology Letters*, 3, 280-285, 10.1021/acs.estlett.6b00152, 2016.
- Kurtén, T., Tiusanen, K., Roldin, P., Rissanen, M., Luy, J.-N., Boy, M., Ehn, M., and Donahue, N.: α -Pinene Autoxidation Products May Not Have Extremely Low Saturation Vapor Pressures Despite High O:C Ratios, *The Journal of Physical Chemistry A*, 120, 2569-2582, 10.1021/acs.jpca.6b02196, 2016.

- Lee, B. H., Mohr, C., Lopez-Hilfiker, F. D., Lutz, A., Hallquist, M., Lee, L., Romer, P., Cohen, R. C., Iyer, S., Kurtén, T., Hu, W., Day, D. A., Campuzano-Jost, P., Jimenez, J. L., Xu, L., Ng, N. L., Guo, H., Weber, R. J., Wild, R. J., Brown, S. S., Koss, A., de Gouw, J., Olson, K., Goldstein, A. H., Seco, R., Kim, S., McAvey, K., Shepson, P. B., Starn, T., Baumann, K., Edgerton, E. S., Liu, J., Shilling, J. E., Miller, D. O., Brune, W., Schobesberger, S., D'Ambro, E. L., and Thornton, J. A.: Highly functionalized organic nitrates in the southeast United States: Contribution to secondary organic aerosol and reactive nitrogen budgets, *Proceedings of the National Academy of Sciences*, 113, 1516-1521, 10.1073/pnas.1508108113, 2016.
- McFiggans, G., Mentel, T. F., Wildt, J., Pullinen, I., Kang, S., Kleist, E., Schmitt, S., Springer, M., Tillmann, R., Wu, C., Zhao, D., Hallquist, M., Faxon, C., Le Breton, M., Hallquist, A. M., Simpson, D., Bergstrom, R., Jenkin, M. E., Ehn, M., Thornton, J. A., Alfarra, M. R., Bannan, T. J., Percival, C. J., Priestley, M., Topping, D., and Kiendler-Scharr, A.: Secondary organic aerosol reduced by mixture of atmospheric vapours, *Nature*, 565, 587-593, 10.1038/s41586-018-0871-y, 2019.
- McGraw, R., and Zhang, R.: Multivariate analysis of homogeneous nucleation rate measurements. Nucleation in the p-toluic acid/sulfuric acid/water system, *The Journal of chemical physics*, 128, 064508, 10.1063/1.2830030, 2008.
- Mentel, T. F., Springer, M., Ehn, M., Kleist, E., Pullinen, I., Kurtén, T., Rissanen, M., Wahner, A., and Wildt, J.: Formation of highly oxidized multifunctional compounds: autoxidation of peroxy radicals formed in the ozonolysis of alkenes – deduced from structure–product relationships, *Atmos. Chem. Phys.*, 15, 6745-6765, 10.5194/acp-15-6745-2015, 2015.
- Mohr, C., Lopez-Hilfiker, F. D., Yli-Juuti, T., Heitto, A., Lutz, A., Hallquist, M., D'Ambro, E. L., Rissanen, M. P., Hao, L. Q., Schobesberger, S., Kulmala, M., Mauldin, R. L., Makkonen, U., Sipila, M., Petaja, T., and Thornton, J. A.: Ambient observations of dimers from terpene oxidation in the gas phase: Implications for new particle formation and growth, *Geophys Res Lett*, 44, 2958-2966, 10.1002/2017gl072718, 2017.
- Molteni, U., Bianchi, F., Klein, F., El Haddad, I., Frege, C., Rossi, M. J., Dommen, J., and Baltensperger, U.: Formation of highly oxygenated organic molecules from aromatic compounds, *Atmospheric Chemistry and Physics*, 18, 1909-1921, 10.5194/acp-18-1909-2018, 2018.
- Paulsen, D., Dommen, J., Kalberer, M., Prevot, A. S., Richter, R., Sax, M., Steinbacher, M., Weingartner, E., and Baltensperger, U.: Secondary organic aerosol formation by irradiation of 1,3,5-trimethylbenzene-NO_x-H₂O in a new reaction chamber for atmospheric chemistry and physics, *Environ Sci Technol*, 39, 2668-2678, 10.1021/es0489137, 2005.
- Rodigast, M., Mutzel, A., and Herrmann, H.: A quantification method for heat-decomposable methylglyoxal oligomers and its application on 1,3,5-trimethylbenzene SOA, *Atmos. Chem. Phys.*, 17, 3929-3943, 10.5194/acp-17-3929-2017, 2017.
- Sato, K., Takami, A., Kato, Y., Seta, T., Fujitani, Y., Hikida, T., Shimono, A., and Imamura, T.: AMS and LC/MS analyses of SOA from the photooxidation of benzene and 1,3,5-trimethylbenzene in the presence of NO_x: effects of chemical structure on SOA aging, *Atmos. Chem. Phys.*, 12, 4667-4682, 10.5194/acp-12-4667-2012, 2012.
- Shrivastava, M., Cappa, C. D., Fan, J. W., Goldstein, A. H., Guenther, A. B., Jimenez, J. L., Kuang, C., Laskin, A., Martin, S. T., Ng, N. L., Petaja, T., Pierce, J. R., Rasch, P. J., Roldin, P., Seinfeld, J. H., Shilling, J., Smith, J. N., Thornton, J. A., Volkamer, R., Wang, J., Worsnop, D. R., Zaveri, R. A., Zelenyuk, A., and Zhang, Q.: Recent advances in understanding secondary organic aerosol: Implications for global climate forcing, *Rev. Geophys.*, 55, 509-559, 10.1002/2016rg000540, 2017.
- Trostl, J., Chuang, W. K., Gordon, H., Heinritzi, M., Yan, C., Molteni, U., Ahlm, L., Frege, C., Bianchi, F., Wagner, R., Simon, M., Lehtipalo, K., Williamson, C., Craven, J. S., Duplissy, J., Adamov, A., Almeida, J., Bernhammer, A. K., Breitenlechner, M., Brilke, S., Dias, A., Ehrhart, S., Flagan, R. C., Franchin, A., Fuchs, C., Guida, R., Gysel, M., Hansel, A., Hoyle, C. R., Jokinen, T., Junninen, H., Kangasluoma, J., Keskinen, H., Kim, J., Krapf, M., Kurten, A., Laaksonen, A., Lawler, J., Leiminger, M., Mathot, S., Mohler, O., Nieminen, T., Onnela, A., Petaja, T., Piel, F. M., Miettinen, P., Rissanen, M. P., Rondo, L., Sarnela, N., Schobesberger, S., Sengupta, K., Sipilaa, M., Smith, J. N., Steiner, G., Tome, A., Virtanen, A., Wagner, A. C., Weingartner, E., Wimmer, D., Winkler, P. M., Ye, P. L., Carslaw, K. S., Curtius, J., Dommen, J., Kirkby, J., Kulmala, M., Riipinen, I., Worsnop, D. R., Donahue, N. M., and Baltensperger, U.: The role of low-volatility organic compounds in initial particle growth in the atmosphere, *Nature*, 533, 527+, 10.1038/nature18271, 2016.
- Wang, S., Wu, R., Berndt, T., Ehn, M., and Wang, L.: Formation of Highly Oxidized Radicals and Multifunctional Products from the Atmospheric Oxidation of Alkylbenzenes, *Environ Sci Technol*, 51, 8442-8449, 10.1021/acs.est.7b02374, 2017.
- Watne, Å. K., Psichoudaki, M., Ljungström, E., Le Breton, M., Hallquist, M., Jerksjö, M., Fallgren, H., Jutterström, S., and Hallquist, Å. M.: Fresh and Oxidized Emissions from In-Use Transit Buses Running on Diesel, Biodiesel, and CNG, *Environmental science & technology*, 52, 7720-7728, 10.1021/acs.est.8b01394, 2018.
- Vereecken, L., and Peeters, J.: A structure–activity relationship for the rate coefficient of H-migration in substituted alkoxy radicals, 10.1039/C0CP00387E, 2010.
- WHO: Ambient air pollution: A global assessment of exposure and burden of disease, 2016.
- Wyche, K. P., Monks, P. S., Ellis, A. M., Cordell, R. L., Parker, A. E., Whyte, C., Metzger, A., Dommen, J., Duplissy, J., Prevot, A. S. H., Baltensperger, U., Rickard, A. R., and Wulfert, F.: Gas phase precursors to anthropogenic secondary organic aerosol: detailed observations of 1,3,5-trimethylbenzene photooxidation, *Atmos. Chem. Phys.*, 9, 635-665, DOI 10.5194/acp-9-635-2009, 2009.
- Yan, C., Nie, W., Aijala, M., Rissanen, M. P., Canagaratna, M. R., Massoli, P., Junninen, H., Jokinen, T., Sarnela, N., Hame, S. A. K., Schobesberger, S., Canonaco, F., Yao, L., Prevot, A. S. H., Petaja, T., Kulmala, M., Sipilaa, M., Worsnop, D. R., and Ehn, M.: Source characterization of highly oxidized multifunctional compounds in a boreal forest environment using positive matrix factorization, *Atmos. Chem. Phys.*, 16, 12715-12731, 10.5194/acp-16-12715-2016, 2016.
- Zhao, Y., Thornton, J. A., and Pye, H. O. T.: Quantitative constraints on autoxidation and dimer formation from direct probing of monoterpene-derived peroxy radical chemistry, *Proc. Natl. Acad. Sci. U. S. A.*, 115, 12142-12147, 10.1073/pnas.1812147115, 2018.

Supplemental Information

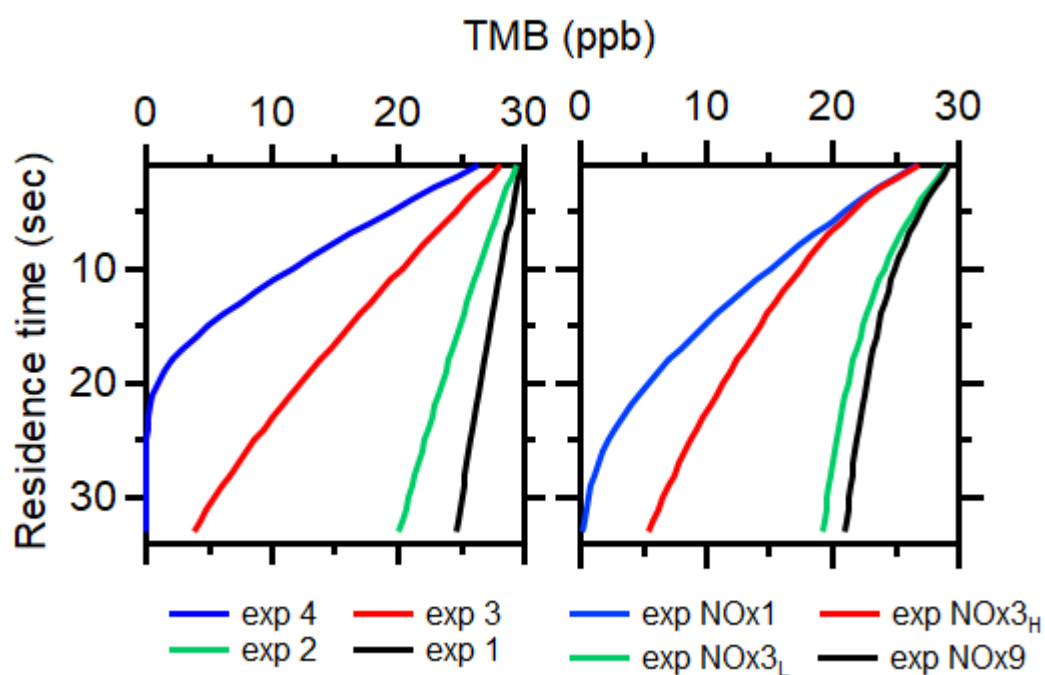
“Effect of NO_x on 1,3,5-trimethylbenzene (TMB) oxidation product distribution and particle formation”

[Epameinondas Tsiligiannis¹](#), [Julia Hammes¹](#), [Christian Mark Salvador¹](#), [Thomas F. Mentel^{1,2}](#), [Mattias Hallquist^{1*}](#)

¹Department of Chemistry and Molecular Biology, University of Gothenburg, Gothenburg, Sweden

²Institute of Energy and Climate Research, IEK-8: Troposphere, Forschungszentrum Jülich GmbH, Jülich, Germany

[Julia Hammes](#), [Epameinondas Tsiligiannis](#), [Thomas Mentel](#), [Mattias Hallquist](#)



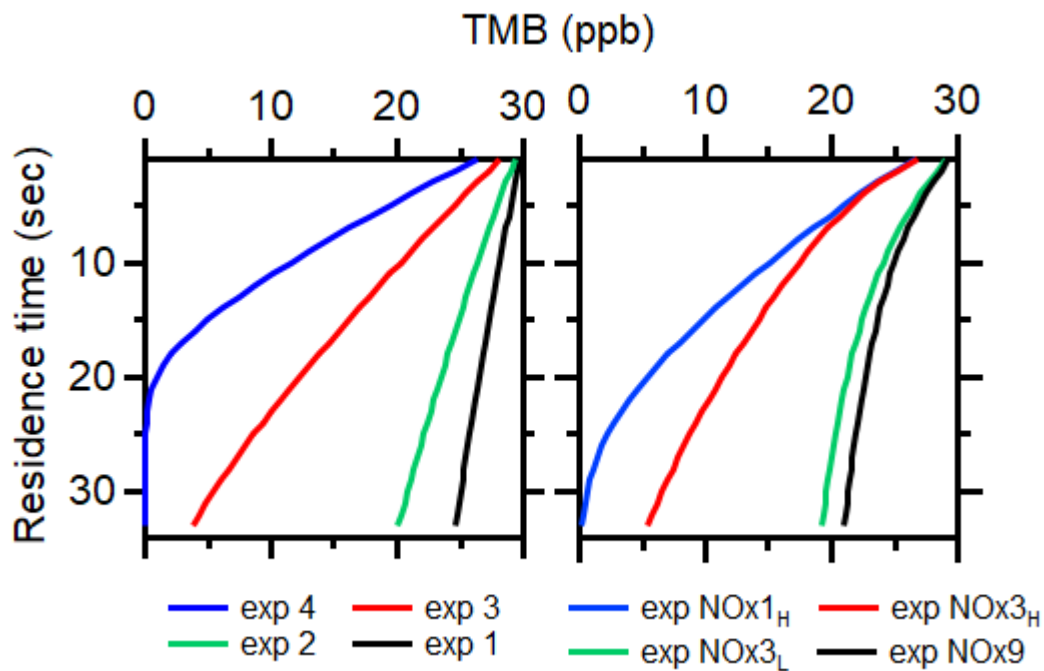


Figure S1: ~~Top:~~ Vertical profile of TMB (ppb) in the PAM chamber without (left) and with NO_x (right). ~~Bottom: Modelled product distribution for all 8 experiments. Left panels show experiments without NO_x and the right panels experiments with NO_x.~~

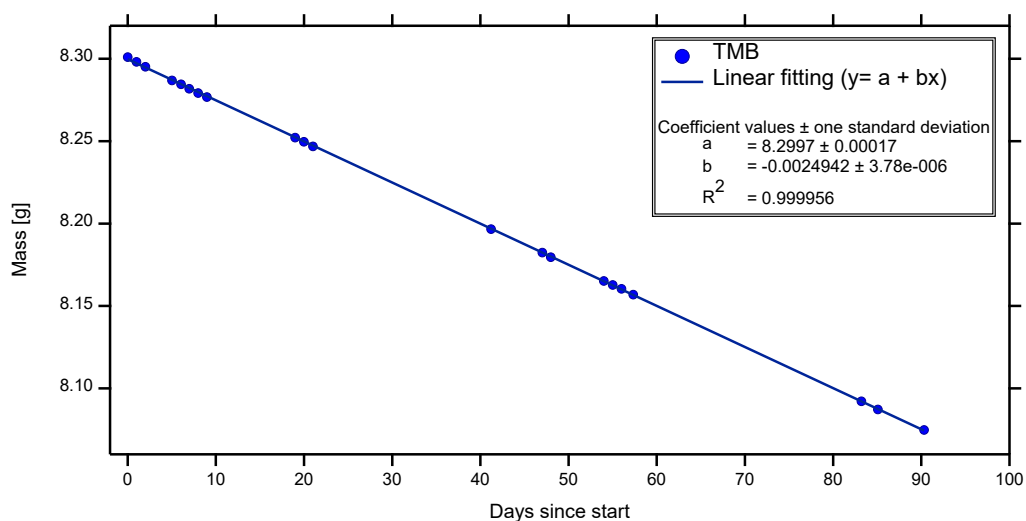


Figure S2: Characterization of TMB evaporation rate from the diffusion vial at a temperature of 20°C.

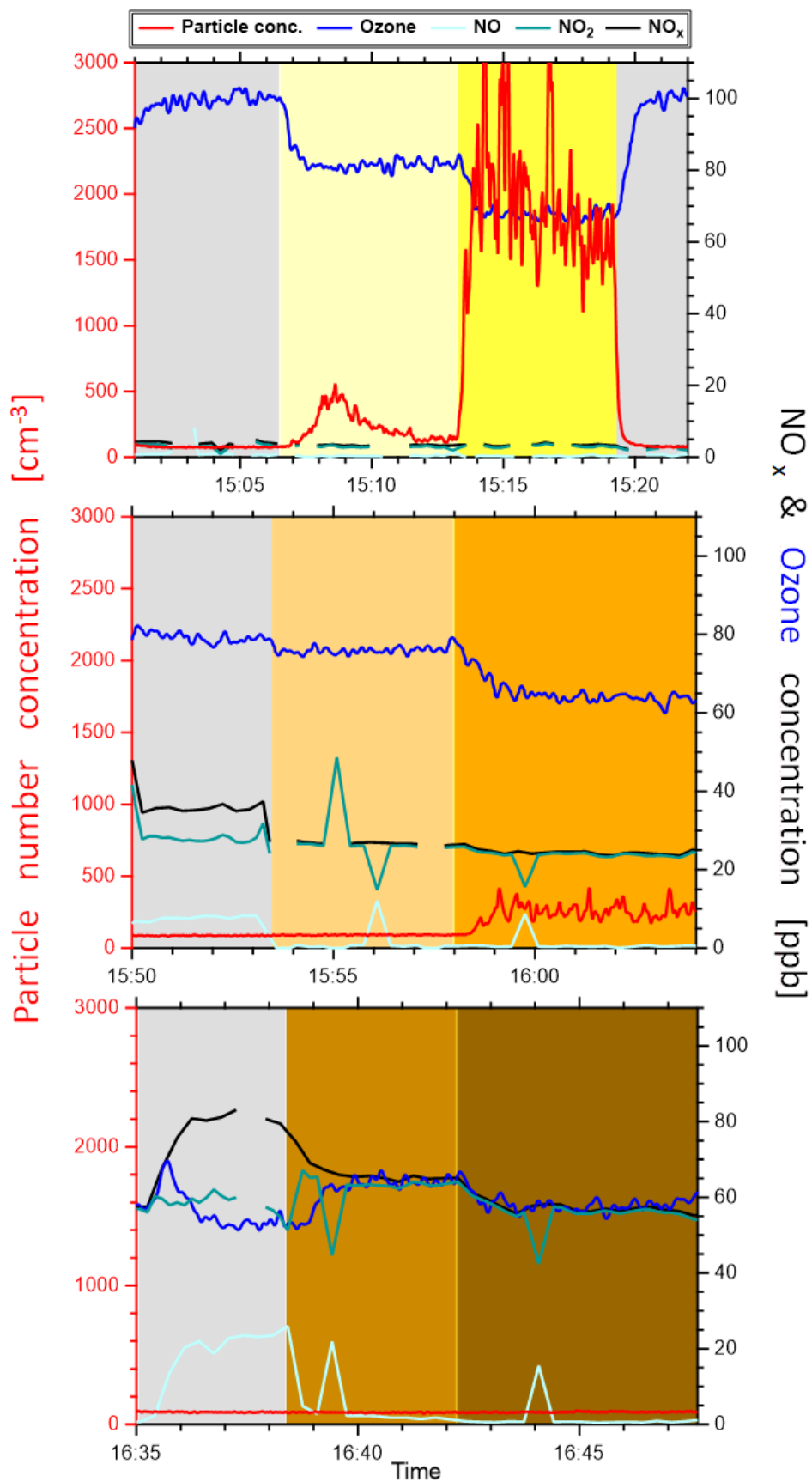


Figure S3: Particle number (red), ozone (blue), NO_x (black), NO (light blue) and NO₂ (cyan) concentrations under NO_x free conditions (top panel), initial NO_x:VOC≈1 (middle panel) and

NO_x:VOC≈3 (bottom panel). The grey areas represent dark conditions, the light yellow, orange and brown represent lower OH exposure conditions (only using one UV lamp is on in the Co:PAM) and the dark yellow, orange and brown represent higher OH exposure conditions (both using two UV lamps are on in the Co:PAM).

Table S1: Contribution of the highest 10 compounds depending on experimental condition.

1		2		3		4	
C ₉ H ₁₂ O ₁₀	4.44	C ₁₈ H ₂₆ O ₁₀	4.76	C ₁₈ H ₂₆ O ₁₀	5.68	C ₉ H ₁₄ O ₇	5.48
C ₁₈ H ₂₆ O ₁₀	4.04	C ₁₈ H ₂₈ O ₁₁	4.53	C ₁₈ H ₂₈ O ₁₁	4.86	C ₉ H ₁₆ O ₉	4.64
C ₁₈ H ₂₈ O ₁₁	3.46	C ₉ H ₁₅ O ₈	3.83	C ₁₈ H ₂₈ O ₁₂	4.55	C ₉ H ₁₄ O ₈	4.49
C ₉ H ₁₅ NO ₁₀	3.07	C ₉ H ₁₄ O ₇	3.19	C ₉ H ₁₄ O ₇	4.27	C ₉ H ₁₆ O ₈	4.48
C ₉ H ₁₃ NO ₈	2.87	C ₉ H ₁₄ O ₈	3.04	C ₉ H ₁₆ O ₈	4.02	C ₁₈ H ₂₈ O ₁₂	3.60
C ₉ H ₁₅ O ₈	2.87	C ₉ H ₁₅ NO ₁₀	2.93	C ₉ H ₁₆ O ₉	3.70	C ₉ H ₁₄ O ₆	3.10
C ₉ H ₁₄ O ₈	2.82	C ₉ H ₁₂ O ₁₀	2.62	C ₉ H ₁₄ O ₈	3.31	C ₉ H ₁₄ O ₉	2.91
C ₉ H ₁₂ O ₉	2.30	C ₉ H ₁₆ O ₈	2.42	C ₉ H ₁₅ O ₈	2.94	C ₉ H ₁₆ O ₇	2.85
C ₁₈ H ₂₅ O ₁₃	2.13	C ₉ H ₁₅ O ₇	2.20	C ₉ H ₁₆ O ₇	2.69	C ₁₈ H ₂₆ O ₁₀	2.84
C ₉ H ₁₅ NO ₈	2.11	C ₉ H ₁₆ O ₉	2.18	C ₁₈ H ₂₆ O ₁₂	2.64	C ₁₈ H ₂₆ O ₁₂	2.68
total	28.6		29.8		38.7		35.9
NO_x3_L		NO_x9		NO_x1		NO_x3_H	
C ₉ H ₁₄ N ₂ O ₁₀	10.0	C ₉ H ₁₄ N ₂ O ₁₀	16.0	C ₉ H ₁₅ NO ₁₀	6.1	C ₉ H ₁₅ NO ₁₀	10.4
C ₉ H ₁₃ NO ₇	7.0	C ₉ H ₁₃ NO ₇	15.6	C ₉ H ₁₄ O ₇	3.7	C ₉ H ₁₄ N ₂ O ₁₀	5.8
C ₉ H ₁₅ NO ₈	6.6	C ₉ H ₁₃ NO ₈	6.1	C ₉ H ₁₆ O ₉	3.4	C ₉ H ₁₃ NO ₈	3.9
C ₉ H ₁₃ NO ₈	5.2	C ₉ H ₁₂ O ₁₀	3.1	C ₉ H ₁₄ O ₈	3.4	C ₉ H ₁₅ NO ₈	2.4
C ₉ H ₁₂ O ₁₀	4.0	C ₉ H ₁₃ NO ₉	2.4	C ₉ H ₁₆ O ₈	3.0	C ₉ H ₁₄ O ₇	2.2
C ₉ H ₁₄ O ₈	2.1	C ₉ H ₁₅ NO ₁₀	2.3	C ₉ H ₁₄ O ₆	2.5	C ₉ H ₁₄ O ₈	2.1
C ₉ H ₁₅ NO ₈	2.1	C ₉ H ₁₂ O ₉	1.9	C ₉ H ₁₄ O ₉	2.3	C ₉ H ₁₃ NO ₉	2.0
C ₉ H ₁₃ NO ₉	2.0	C ₉ H ₁₄ O ₈	1.8	C ₁₈ H ₂₈ O ₁₂	2.1	C ₉ H ₁₄ O ₆	2.0
C ₉ H ₁₂ O ₉	1.8	C ₉ H ₁₄ N ₂ O ₉	1.7	C ₉ H ₁₅ O ₈	2.0	C ₉ H ₁₂ O ₁₀	1.8
C ₉ H ₁₃ NO ₈	1.7	C ₉ H ₁₃ NO ₁₀	1.6	C ₁₈ H ₂₆ O ₁₀	1.9	C ₉ H ₁₃ NO ₇	1.6
total	42.3		52.4		30.5		34.2

Kinetic model of HOM and ON formation in PAM chamber

A chemical model, describing comprehensively the ozone photolysis at 254nm and NO_x chemistry as well as the general scheme for HOM formation by 1,3,5 trimethylbenzene (TMB) in the Go:PAM, was used. The main structure of the model is based on Watne et al. (2018), where the rate coefficients are adapted from Sander et al. (2011) and Li et al. (2015). The new NO_x chemistry are based on Atkinson et al. (1992); Finlayson-Pitts (1999) and Berndt et al. (2018), while the regular TMB oxidation scheme was taken from the MCM v3.3.1 (Jenkin et al., 2003) and the more oxidized one from Ehn et al. (2014); Wang et al. (2017); Jenkin et al. (2019); Berndt et al. (2018) and Zhao et al. (2018). All the reaction and the corresponding rate constants are given in Table S2. FACSIMILE 4 (FACSIMILE for Windows 4, 2009) was used to implement the model and solve the ordinary differential equations.

The photon flux at 254nm used in the simulations was tuned to match measured decay of O₃ and was calculated to be $P_{\text{FLUX}254} = 1.31 \times 10^{16} \text{ cm}^{-2}\text{s}^{-1}$. A OH sink was added to match the observed OH production in the background experiment, i.e. without the addition of TMB. The model was run for all experiments with and without NO_x. HOM (MONOMER) were produced as a termination product from HOMRO₂ or the corresponding alkoxy radical (HOMRO). According to the oxygen content in the majority of the C₉ products the oxidized peroxy radicals (HOMRO₂) should contain either seven, nine or eleven oxygen atoms which would be formed after two, three and/or four autoxidation steps, respectively. To simplify the model the produced HOMRO₂ in the model were assumed considered to be formed after 3 autoxidation steps. There are large uncertainties on estimating these rate coefficients for the autoxidation step (Jenkin et al., 2019). The following assumptions were taken in account for our best lumped estimation of the three step oxidation. The 1st step where the O₂ group make a bicyclic radical most likely has a large rate coefficient where Jenkin et al., 2019 suggests a rate coefficient for similar reactions to be larger than $3.6 \times 10^2 \text{ s}^{-1}$ (Jenkin et al., 2019). For the 2nd step we assume an internal hydrogen shift potentially facilitated by a conjugated three carbon system. Here Wang et al., 2017 give a large range in reaction rates for similar reactions where the radical from toluene is slow ($2.6 \times 10^{-2} \text{ s}^{-1}$) while the radical from larger compounds has higher values (e.g. 7.0 s^{-1}). We use a value of 1 s^{-1} to represent this 2nd step. For the 3rd step that would represent another hydrogen shift we use the value of 0.5 s^{-1} originally suggested in the paper by Ehn et al., 2014. The combined rate of these three subsequent steps would then be 0.33 s^{-1} . (Ehn et al., 2014) of a general RO₂ with a rate constant of 0.1667 s^{-1} . The oxidation state of produced dimers was defined as low, medium or high, depending on the cross reactions. A cross reaction between a general RO₂ and another RO₂ leads to low oxidized dimer (LODIMER), between a RO₂ and HOMRO₂ leads to medium oxidized dimer (MODIMER) and between a HOMRO₂ and another HOMRO₂ leads to high oxidized dimer (HODIMER). Highly oxygenated nitrates (ON) was formed via HOMRO₂ reaction with NO.

Three different cases were tested, in which the rate coefficients of the cross reactions (Reactions 63 – 68) were varied. During the 1st case the rate coefficients of the following reactions (Reactions 63, 64, 66 and 67) was $8.8 \times 10^{-13} \text{ cm}^3 \text{ molecules}^{-1} \text{ s}^{-1}$ (MCM) and the dimer formation reactions (Reactions 65 and 68) were based on Berndt et al. (2018). In that case either we overestimate the production of dimers, underestimate the production of monomers or both of them. The concentration of dimers dominates even in the experiments with high NO_x, which is not consistent with our measurements. In the 2nd case the rate coefficient of Reactions 65 and 68 were kept constant, but for the rest of them changed to $1 \times 10^{-12} \text{ cm}^3 \text{ molecules}^{-1} \text{ s}^{-1}$ based on Zhao et al. (2018). The concentration of the dimers was still quite higher than the monomers and nitrates, even in the high NO_x experiments. This overestimation suggests that the rate coefficients of the reactions, in which dimers are produced, are lower. Thus, during the 3rd case the rate coefficients for the reactions 65 and 68 were decreased to $2 \times 10^{-12} \text{ cm}^3 \text{ molecules}^{-1} \text{ s}^{-1}$ (Zhao et al., 2018). The same value was used for both dimer formation reactions, in contrast to the 1st and 2nd cases. The 3rd case gives the best results compared to our measurements (see main text).

Table S2: Reactions and rate coefficients for model calculations. Rate constants were taken from Sander et al. (2011), Li et al. (2015), and Jenkin et al., (2013,2003) unless otherwise stated. The temperature was 298 K, the relative humidity was 38% and the pressure ($M = 2.46 \times 10^{19}$ molecules cm^{-3}).

No.	Reaction	k	Comments
1	$\text{O}_3 + \text{h}\nu \rightleftharpoons \text{O}_2 + \text{O}(1\text{D})$	0.15	$\sigma_{254} = 1.148 \times 10^{-17} \text{cm}^{-2}$
2	$\text{O}(1\text{D}) + \text{H}_2\text{O} \rightleftharpoons \text{OH} + \text{OH}$	1.99×10^{-10}	
3	$\text{O}(1\text{D}) + \text{O}_2 \rightleftharpoons \text{O}(3\text{P}) + \text{O}_2$	3.97×10^{-11}	
4	$\text{O}(1\text{D}) + \text{O}_3 \rightleftharpoons \text{O}_2 + \text{O}(3\text{P}) + \text{O}(3\text{P})$	1.2×10^{-10}	
5	$\text{O}(1\text{D}) + \text{O}_3 \rightleftharpoons \text{O}_2 + \text{O}_2$	1.2×10^{-10}	
6	$\text{O}(1\text{D}) + \text{N}_2 \rightleftharpoons \text{O}(3\text{P}) + \text{N}_2$	3.11×10^{-11}	
7	$\text{O}(3\text{P}) + \text{O}_2 + \text{M} \rightleftharpoons \text{O}_3 + \text{M}$	6.1×10^{-34}	
8	$\text{O}(3\text{P}) + \text{O}_3 \rightleftharpoons \text{O}_2 + \text{O}_2$	7.96×10^{-15}	
9	$\text{O}(3\text{P}) + \text{OH} \rightleftharpoons \text{H} + \text{O}_2$	3.29×10^{-11}	
10	$\text{H} + \text{O}_2 \rightleftharpoons \text{HO}_2$	9.57×10^{-13}	
11	$\text{H} + \text{HO}_2 \rightleftharpoons \text{OH} + \text{OH}$	7.2×10^{-11}	
12	$\text{H} + \text{HO}_2 \rightleftharpoons \text{O}(3\text{P}) + \text{H}_2\text{O}$	1.6×10^{-12}	
13	$\text{H} + \text{HO}_2 \rightleftharpoons \text{H}_2 + \text{O}_2$	6.9×10^{-12}	
14	$\text{OH} + \text{OH} \rightleftharpoons \text{H}_2\text{O} + \text{O}(3\text{P})$	1.8×10^{-12}	
15	$\text{OH} + \text{OH} \rightleftharpoons \text{H}_2\text{O}_2$	6.29×10^{-12}	
16	$\text{OH} + \text{O}_3 \rightleftharpoons \text{HO}_2 + \text{O}_2$	7.25×10^{-14}	
17	$\text{HO}_2 + \text{HO}_2 \rightleftharpoons \text{H}_2\text{O}_2 + \text{O}_2$	3.28×10^{-12}	$(k_{17} = 3 \times 10^{-13} \times e^{(460/T)} + 2.1 \times 10^{-33} \times e^{(920/T)} \times M) \times (1 + 1.4 \times 10^{-21}) \times \text{H}_2\text{O} \times e^{(2200/T)}$
18	$\text{OH} + \text{TMB} \rightleftharpoons 0.82 \text{RO}_2$	5.67×10^{-11}	MCM
19	$\text{OH} + \text{TMB} \rightleftharpoons 0.18 \text{HO}_2$	5.67×10^{-11}	MCM
20	$\text{NO} + \text{O}(3\text{P}) \rightleftharpoons \text{NO}_2$	1.66×10^{-12}	
21	$\text{O}(3\text{P}) + \text{OH} \rightleftharpoons \text{H} + \text{O}_2$	3.29×10^{-11}	
22	$\text{NO}_2 + \text{h}\nu \rightleftharpoons \text{NO} + \text{O}(3\text{P})$	1.37×10^{-4}	$\sigma_{254} = 1.05 \times 10^{-20}$
23	$\text{OH} + \text{NO}_2 \rightleftharpoons \text{HNO}_3$	1.06×10^{-11}	
24	$\text{OH} + \text{NO}_2 \rightleftharpoons \text{HOONO}$	1.79×10^{-12}	
25	$\text{HO}_2 + \text{NO} \rightleftharpoons \text{OH} + \text{NO}_2$	8.16×10^{-12}	
26	$\text{RO}_2 + \text{NO} \rightleftharpoons \text{RO} + \text{NO}_2$	9.0×10^{-12}	MCM
27	$\text{O}(1\text{D}) + \text{N}_2 + \text{M} \rightleftharpoons \text{N}_2\text{O} + \text{M}$	2.82×10^{-36}	
28	$\text{N}_2\text{O} + \text{O}(1\text{D}) \rightleftharpoons \text{N}_2 + \text{O}_2$	5.09×10^{-11}	
29	$\text{N}_2\text{O} + \text{O}(1\text{D}) \rightleftharpoons \text{NO} + \text{NO}$	7.64×10^{-11}	
30	$\text{O}(3\text{P}) + \text{HO}_2 \rightleftharpoons \text{OH} + \text{O}_2$	5.87×10^{-11}	
31	$\text{O}(3\text{P}) + \text{H}_2\text{O}_2 \rightleftharpoons \text{OH} + \text{HO}_2$	1.7×10^{-15}	
32	$\text{H} + \text{O}_3 \rightleftharpoons \text{OH} + \text{O}_2$	2.89×10^{-11}	
33	$\text{HO}_2 + \text{O}_3 \rightleftharpoons \text{OH} + \text{O}_2 + \text{O}_2$	1.93×10^{-15}	
34	$\text{HO}_2 + \text{OH} \rightleftharpoons \text{H}_2\text{O} + \text{O}_2$	1.11×10^{-10}	
35	$\text{H}_2\text{O}_2 + \text{h}\nu \rightleftharpoons \text{OH} + \text{OH}$	8.75×10^{-4}	$\sigma_{254} = 6.7 \times 10^{-20}$
36	$\text{HO}_2 + \text{h}\nu \rightleftharpoons \text{OH} + \text{O}(1\text{D})$	3.4×10^{-4}	$\sigma_{254} = 2.6 \times 10^{-19}$
37	$\text{H}_2\text{O}_2 + \text{OH} \rightleftharpoons \text{HO}_2 + \text{H}_2\text{O}$	1.8×10^{-12}	
38	$\text{NO} + \text{O}_3 \rightleftharpoons \text{NO}_2 + \text{O}_2$	1.95×10^{-14}	
39	$\text{O}(1\text{D}) + \text{H}_2 \rightleftharpoons \text{OH} + \text{H}$	1.2×10^{-10}	

40	$\text{OH} + \text{H}_2 \rightleftharpoons \text{H}_2\text{O} + \text{H}$	6.67×10^{-15}	
41	$\text{NO}_2 + \text{O}(3\text{P}) \rightleftharpoons \text{NO} + \text{O}_2$	1.03×10^{-11}	
42	$\text{NO}_2 + \text{O}(3\text{P}) \rightleftharpoons \text{NO}_3$	1.61×10^{-12}	
43	$\text{H} + \text{NO}_2 \rightleftharpoons \text{NO} + \text{OH}$	1.28×10^{-10}	
44	$\text{NO} + \text{NO}_3 \rightleftharpoons \text{NO}_2 + \text{NO}_2$	2.65×10^{-11}	
45	$\text{NO}_2 + \text{O}_3 \rightleftharpoons \text{NO}_3 + \text{O}_2$	3.2×10^{-17}	
46	OH deposition/loss	2.685	
47	$\text{RO}_2 + \text{HO}_2 \rightleftharpoons \text{ROOH} + \text{O}_2$	2.28×10^{-11}	MCM
48	$\text{RO}_2 + \text{RO}_2 \rightleftharpoons 0.38 (\text{Carbonyl} + \text{Alcohol} + \text{O}_2)$	8.8×10^{-13}	MCM
49	$\text{RO}_2 + \text{RO}_2 \rightleftharpoons 0.58 (\text{RO} + \text{RO} + \text{O}_2)$	8.8×10^{-13}	MCM
50	$\text{RO}_2 + \text{RO}_2 \rightleftharpoons 0.04 (\text{LODIMER} + \text{O}_2)$	8.8×10^{-13}	Low Oxidized dimer, MCM, Zhao et al. (2018)
51	$\text{RO}_2 + \text{NO}_2 \rightleftharpoons \text{RO}_2\text{NO}_2$	9.0×10^{-12}	p 187 Finlayson - Pitts & Pitts (2000)
52	$\text{RO}_2 \rightleftharpoons \text{HOMRO}_2$	$0.16670.33$	3 steps, Jenkin et al (2019); Wang et al. (2017); Ehn et al. (2018, 2014)
53	$\text{RO} \rightleftharpoons 0.3 (\text{Carbonyl} + \text{HO}_2)$	1.0×10^{-6}	MCM, Fraction is empirically determined
54	$\text{RO} \rightleftharpoons 0.7 \text{RO}_2$	1.0×10^{-6}	MCM, Fraction is empirically determined
55	$\text{HOMRO}_2 + \text{HO}_2 \rightleftharpoons \text{MONOMER}$	2.28×10^{-11}	MCM
56	$\text{HOMRO}_2 + \text{NO} \rightleftharpoons 0.3 \text{ONs}$	1.0×10^{-11}	Berndt et al. (2018)
57	$\text{HOMRO}_2 + \text{NO} \rightleftharpoons 0.7 (\text{HOMRO} + \text{NO}_2)$	1.0×10^{-11}	Berndt et al. (2018)
58	$\text{HOMRO} \rightleftharpoons 0.3 (\text{MONOMER} + \text{HO}_2)$	1.0×10^{-6}	MCM, Fraction is empirically determined
59	$\text{HOMRO} \rightleftharpoons 0.7 \text{HOMRO}_2$	1.0×10^{-6}	MCM, Fraction is empirically determined
60	$\text{HOMRO}_2 + \text{NO}_2 \rightleftharpoons \text{HOMRO}_2\text{NO}_2$	9.0×10^{-12}	p 187 Finlayson - Pitts & Pitts (2000)
61	$\text{RO}_2\text{NO}_2 \rightleftharpoons \text{RO}_2 + \text{NO}_2$	3.99	Atkinson et al. (1992)
62	$\text{HOMRO}_2\text{NO}_2 \rightleftharpoons \text{HOMRO}_2 + \text{NO}_2$	3.99	Atkinson et al. (1992)
Case 1			
63	$\text{HOMRO}_2 + \text{RO}_2 \rightleftharpoons 0.4 (\text{MONOMER} + \text{Carbonyl/Alcohol} + \text{O}_2)$	8.8×10^{-13}	MCM
64	$\text{HOMRO}_2 + \text{RO}_2 \rightleftharpoons 0.6 (\text{HOMRO} + \text{RO} + \text{O}_2)$	8.8×10^{-13}	MCM
65	$\text{HOMRO}_2 + \text{RO}_2 \rightleftharpoons \text{MODIMER} + \text{O}_2$	8.0×10^{-11}	Medium Oxidized dimer, Berndt et al. (2018)
66	$\text{HOMRO}_2 + \text{HOMRO}_2 \rightleftharpoons 0.4 (\text{MONOMER} + \text{MONOMER} + \text{O}_2)$	8.8×10^{-13}	MCM
67	$\text{HOMRO}_2 + \text{HOMRO}_2 \rightleftharpoons 0.6 (\text{HOMRO} + \text{HOMRO} + \text{O}_2)$	8.8×10^{-13}	MCM
68	$\text{HOMRO}_2 + \text{HOMRO}_2 \rightleftharpoons \text{HODIMER} + \text{O}_2$	2.6×10^{-10}	Highly Oxidized dimer, Berndt et al. (2018)
Case 2			
63	$\text{HOMRO}_2 + \text{RO}_2 \rightleftharpoons 0.4 (\text{MONOMER} + \text{Carbonyl/Alcohol} + \text{O}_2)$	1.0×10^{-12}	Zhao et al. (2018)
64	$\text{HOMRO}_2 + \text{RO}_2 \rightleftharpoons 0.6 (\text{HOMRO} + \text{RO} + \text{O}_2)$	1.0×10^{-12}	Zhao et al. (2018)
65	$\text{HOMRO}_2 + \text{RO}_2 \rightleftharpoons \text{MODIMER} + \text{O}_2$	8.0×10^{-11}	Medium Oxidized dimer, Berndt et al. (2018)
66	$\text{HOMRO}_2 + \text{HOMRO}_2 \rightleftharpoons 0.4 (\text{MONOMER} + \text{MONOMER} + \text{O}_2)$	1.0×10^{-12}	Zhao et al. (2018)
67	$\text{HOMRO}_2 + \text{HOMRO}_2 \rightleftharpoons 0.6 (\text{HOMRO} + \text{HOMRO} + \text{O}_2)$	1.0×10^{-12}	Zhao et al. (2018)

Case 3	68	HOMRO2 + HOMRO2 \rightarrow HODIMER + O2	2.6×10^{-10}	Highly Oxidized dimer, Berndt et al. (2018)
	63	HOMRO2 + RO2 \rightarrow 0.4 (MONOMER + Carbonyl/Alcohol + O2)	1.0×10^{-12}	Zhao et al. (2018)
	64	HOMRO2 + RO2 \rightarrow 0.6 (HOMRO + RO + O2)	1.0×10^{-12}	Zhao et al. (2018)
	65	HOMRO2 + RO2 \rightarrow MODIMER + O2	2.0×10^{-12}	Medium Oxidized dimer, Zhao et al. (2018)
	66	HOMRO2 + HOMRO2 \rightarrow 0.4 (MONOMER + MONOMER + O2)	1.0×10^{-12}	Zhao et al. (2018)
	67	HOMRO2 + HOMRO2 \rightarrow 0.6 (HOMRO + HOMRO + O2)	1.0×10^{-12}	Zhao et al. (2018)
	68	HOMRO2 + HOMRO2 \rightarrow HODIMER + O2	2.0×10^{-12}	Highly Oxidized dimer, Zhao et al. (2018)

References (supplemental)

Atkinson, R., Baulch, D. L., Cox, R. A., Hampson, R. F., Kerr, J. A., and Troe, J.: Evaluated Kinetic and Photochemical Data for Atmospheric Chemistry Supplement-IV - Iupac Subcommittee on Gas Kinetic Data Evaluation for Atmospheric Chemistry, *J Phys Chem Ref Data*, 21, 1125-1568, Doi 10.1063/1.555918, 1992.

Berndt, T., Scholz, W., Mentler, B., Fischer, L., Herrmann, H., Kulmala, M., and Hansel, A.: Accretion Product Formation from Self- and Cross-Reactions of RO2 Radicals in the Atmosphere, *Angewandte Chemie (International ed. in English)*, 57, 3820-3824, 10.1002/anie.201710989, 2018.

Ehn, M., Thornton, J. A., Kleist, E., Sipila, M., Junninen, H., Pullinen, I., Springer, M., Rubach, F., Tillmann, R., Lee, B., Lopez-Hilfiker, F., Andres, S., Acir, I. H., Rissanen, M., Jokinen, T., Schobesberger, S., Kangasluoma, J., Kontkanen, J., Nieminen, T., Kurten, T., Nielsen, L. B., Jorgensen, S., Kjaergaard, H. G., Canagaratna, M., Maso, M. D., Berndt, T., Petaja, T., Wahner, A., Kerminen, V. M., Kulmala, M., Worsnop, D. R., Wildt, J., and Mentel, T. F.: A large source of low-volatility secondary organic aerosol, *Nature*, 506, 476-479, 10.1038/nature13032, 2014.

[FACSIMILE for Windows 4, v. 4.0.48; MCPA Software Ltd: Faringdon, UK, 2009.](#)

Finlayson-Pitts, B. and Pitts, J.: *Chemistry of the Upper and Lower Atmosphere*, [Academic Press](#), 1999.

~~Sander, S. P.; Friedl, R. R.; Barker, J. R.; Golden, D. M.; Kurylo, M. J.; Wine, P. H.; Abbat, J. P. D.; Burkholder, J. P.; Kolb, C. E.; Moortgat, G. K.; Huie, R. E.; Orkin, V. L., *Chemical Kinetics and Photochemical data for Use in Atmospheric Studies*. JPL publication 10-6 2011, 17 (10-6).~~

~~Li, R.; Palm, B. B.; Ortega, A. M.; Hlywiak, J.; Hu, W.; Peng, Z.; Day, D. A.; Knote, C.; Brune, W. H.; de Gouw, J. A.; Jimenez, J. L., *Modeling the Radical Chemistry in an Oxidation Flow Reactor: Radical Formation and Recycling, Sensitivities, and the OH Exposure Estimation Equation*. *The Journal of Physical Chemistry A* 2015, 119, (19), 4418-4432.~~

~~[FACSIMILE for Windows 4, v. 4.0.48; MCPA Software Ltd: Faringdon, UK, 2009.](#)~~

Jenkin, M. E.; Saunders, S. M.; Wagner, V.; Pilling, M. J., Protocol for the development of the Master Chemical Mechanism, MCM v3 (Part B): tropospheric degradation of aromatic volatile organic compounds. *Atmos. Chem. Phys.* 2003, 3, 181-193, 2003.

[Jenkin, M. E.; Valorso, R.; Aumont, B.; Rickard, A.R., *Estimation of rate coefficients and branching ratios for reactions of organic peroxy radicals for use in automated mechanism construction*. *Atmos. Chem. Phys.*, 19, 7671-7717, 2019.](#)

[Li, R.; Palm, B. B.; Ortega, A. M.; Hlywiak, J.; Hu, W.; Peng, Z.; Day, D. A.; Knote, C.; Brune, W. H.; de Gouw, J. A.; Jimenez, J. L., *Modeling the Radical Chemistry in an Oxidation Flow Reactor: Radical Formation and Recycling, Sensitivities, and the OH Exposure Estimation Equation*. *The Journal of Physical Chemistry A* 2015, 119, \(19\), 4418-4432, 2015.](#)

Sander, S. P.; Friedl, R. R.; Barker, J. R.; Golden, D. M.; Kurylo, M. J.; Wine, P. H.; Abbat, J. P. D.; Burkholder, J. P.; Kolb, C. E.; Moortgat, G. K.; Huie, R. E.; Orkin, V. L., Chemical Kinetics and Photochemical data for Use in Atmospheric Studies. JPL publication 10-6-2011, 17 (10-6), 2011.

Wang, S., Wu, R., Berndt, T., Ehn, M., and Wang, L.: Formation of Highly Oxidized Radicals and Multifunctional Products from the Atmospheric Oxidation of Alkylbenzenes, Environ Sci Technol, 51, 8442-8449, 10.1021/acs.est.7b02374, 2017.

Watne, A. K., Psichoudaki, M., Ljungstrom, E., Le Breton, M., Hallquist, M., Jerksjo, M., Fallgren, H., Jutterstrom, S., and Hallquist, A. M.: Fresh and Oxidized Emissions from In-Use Transit Buses Running on Diesel, Biodiesel, and CNG, Environmental science & technology, 52, 7720-7728, 10.1021/acs.est.8b01394, 2018.

Zhao, Y., Thornton, J. A., and Pye, H. O. T.: Quantitative constraints on autoxidation and dimer formation from direct probing of monoterpene-derived peroxy radical chemistry, Proc Natl Acad Sci U S A, 115, 12142-12147, 10.1073/pnas.1812147115, 2018.